Chapter 4

Results of Principal Component Analysis. Daily data. European window.

In order to extend the study to the rest of Europe, the whole analysis has been applied to a new spatial window that it has been extended covering the European domain. The results to be shown correspond to the PCA methodology applied to daily large-scale data for the European window. As with the Iberian case, the databases are seasonally grouped.

Prior to the spatial statistical results, tables with explained variance percentages for the most significant PCs or modes for the large-scale field, described in the previous chapter, are shown. Although the PCA has been applied to large-scale fields of several variables at different atmospheric levels, this delivery will be confined to the near-surface fields, representing the large-scale atmospheric circulation at a more realistic height level, of the circulation patterns associated with the observational wind speed field. In addition, eigenvectors are also shown as well as their links with the most relevant Atlantic atmospheric patterns. Thus, and for reasons of brevity, explanations will be made only for SLP and for winter.

4.1. PCA results of large-scale variables. Meteorological analysis of the first modes of SLP. European window

The following table displays the variance percentages accounted for by the most significant PCs or modes for the sea-level-pressure (SLP) over the European window, already described in previous chapter. The first ten PCs for winter account for more than 70% of total variance of the original data.

Level(hPa)	Component	SLP(var)
SLP	1	21
	2	12
	3	10
	4	7
	5	6
	6	5
	7	4
	8	3
	9	2
	10	1

Table 4.1. Variance percentages of the first ten PCs for sea level pressure in the European window.

The Figure IV-1 shows the eigenvectors or spatial patterns associated with the first ten PCs of the sea level pressure variable covering the European window.

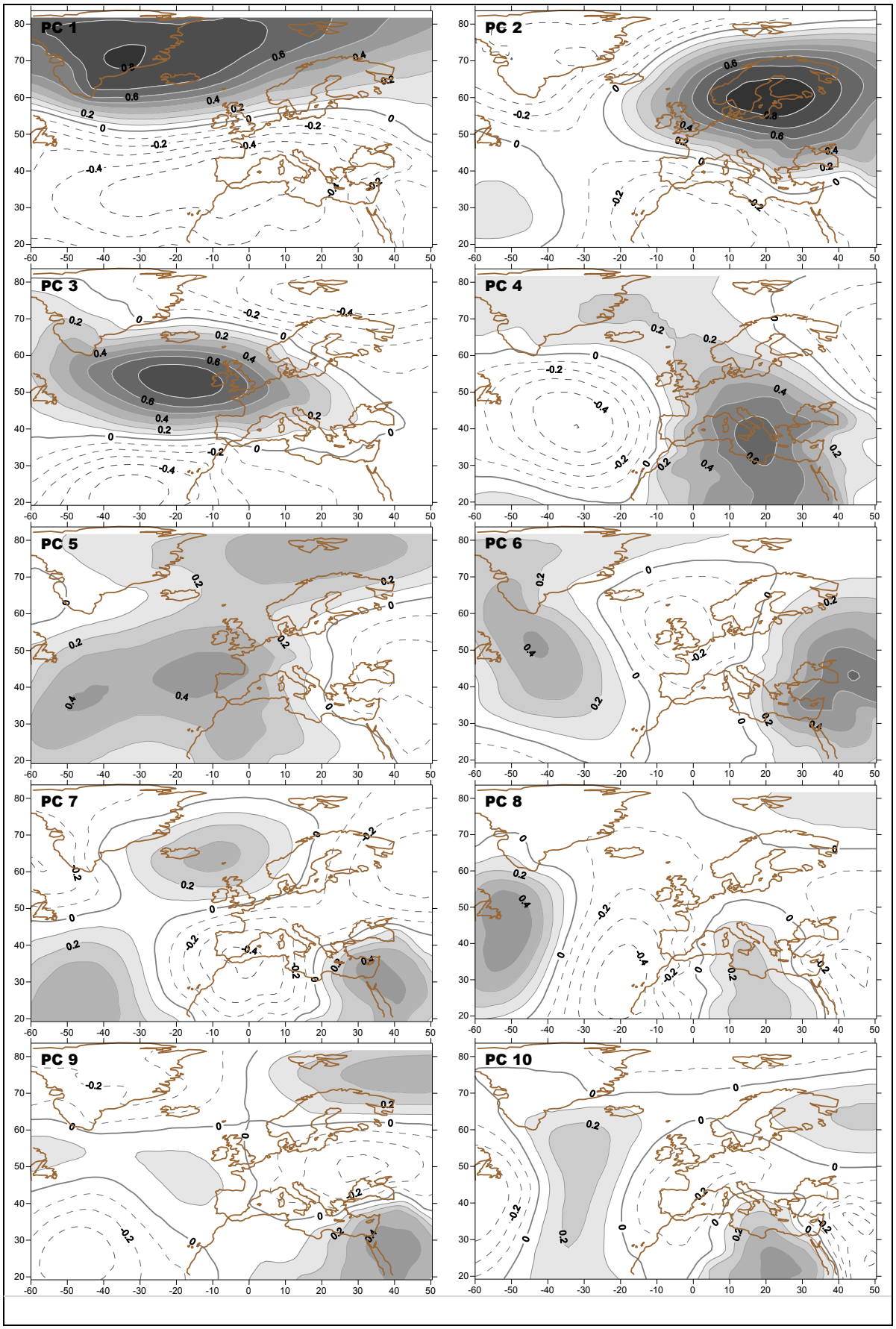

Figure IV-1. The first ten PCA patterns of SLP for winter. Contours indicate correlation values.

In this section the first ten significant modes obtained from the PCA are illustrated in terms of their spatial configurations and their temporal evolutions, describing how the spatial configurations are representative of several Atlantic teleconnection patterns.

First mode

The first mode obtained from the application of the PCA accounts for the main percentage of variance of the original data. Thus, this obtained PC represents the most representative mode. High correlation values can be noticed, the sign of isolines being arbitrary. The SLP pattern, (Figure IV-1) is characterised by a north-south dipole configuration. One of the two centres is located centred over the Iberian Peninsula while the other one is situated east to Greenland. The spatial pattern shows a meridionally gradient similar to the well known North Atlantic Oscillation, NAO, teleconnection pattern (Barnston and Livezey, 1987). This pattern is characterized by below normal pressure across the high latitudes and above normal pressure over the central North Atlantic Ocean, the eastern United States and Western Europe (Barnston and Livezey, 1987).

The intensification of high pressure over the 35ºN promotes extreme westerlies wind across the North Atlantic Ocean and below normal temperatures in the western Greenland while above normal temperatures are promoted over the eastern area of the United States and northern Europe. Additionally positive anomalies of precipitation are observed in the northern Europe and Scandinavian areas while negative ones are located in the southern and central part of Europe (van Loon and Rogers, 1978; Rogers and van Loon, 1979). On the other hand, the intensification of the Iceland low promotes strong southwestern advection favouring maritime air over the European continent.

In Figure IV-2 it can be observed the time evolution of the most significant scores or PC time series associated with the SLP field. In analogous way to the time series of the previous chapter, wavelet transforms have been applied to the PC time series of the SLP field.

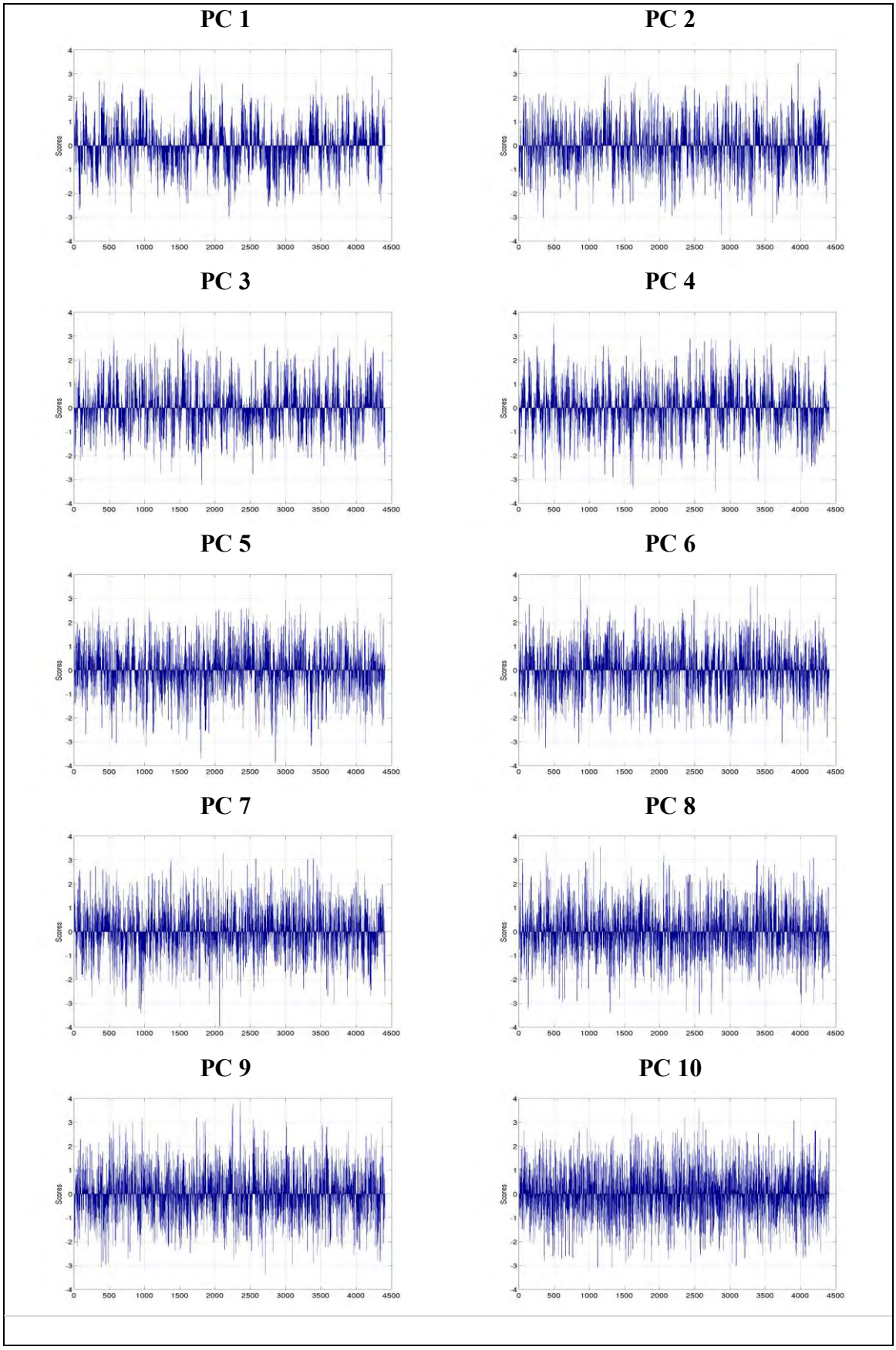

Figure IV-2: Time series of PCs corresponding with the first ten modes of SLP.

The Figure IV-3 displays the wavelet power spectrum displayed as a function of period and time, corresponding to the first PC SLP time series. The magnitude of wavelet coefficients gives a measure of the correlation between the signal and the wavelet basis. The power spectrum associated with the first PC time series of the SLP field is mainly characterized by scales evolving between 5 and 10 years (see y-axis of Figure IV-3), throughout the whole time period (1958 to 2007) showing power spectrum intensity mainly concentrated between 1974-1994 with a noticeable evolution of maximum/minimum nucleus. There are energetic oscillations, mainly negative nuclei, in scales below 3 years, indicating low intra-year and inter-year variability at such periods. Additionally, periodograms of the time series were derived (not shown) to reveal that the maximum power of the spectra is concentrated in periods of less than 10 years, showing similarity with the wavelet results shown.

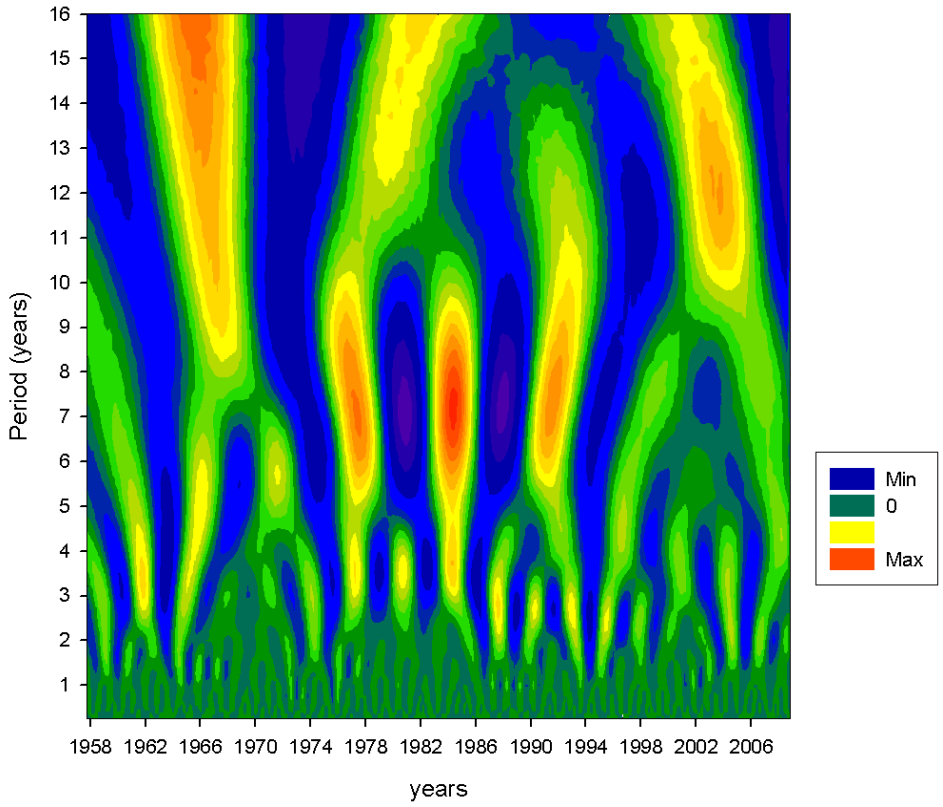

Figure IV-3: The wavelet power spectrum of the SLP time series corresponding to the first PC. The y-axis represents the variability scale (years) and the x-axis corresponds to the time period.

Second mode

The obtained patterns associated with the second mode of the SLP account for the second quantity of variance of the original dada. In a similar way to the first pattern, it can be observed high correlation values in the large-scale field (Figure IV-1). The SLP pattern shows strong resemblance with the Euro Atlantic teleconnection pattern (EU1) identified by Barnston and Livezey (1987) for geopotential height at Z500 hPa. The EU1 was characterized by a principal circulation node extended over the Scandinavian Peninsula and most of the Artic Ocean and northern Siberia with two additional nuclei of opposite sign over southern Europe and western China (Barnston and Livezey, 1987). The SLP pattern obtained from the PCA methodology in the European window presents strong dipolar structure with a centre of high positive anomalies over the Scandinavian area and negative anomalies located over the southern area of study.

Third mode

The third most significant pattern obtained for the SLP field could show a configuration structurally similar to the Barnston and Livezey (1987) for the Z500 hPa identified as East Atlantic (EA) teleconnection pattern, which constitutes the low-frequency second variability mode of the three most significant modes over the North Atlantic Ocean. Such mode consists of a north-south anomaly centre dipole spanning the North Atlantic from east to west. The anomaly centres of the EA pattern are displaced southeastward to the approximate nodal lines of the NAO pattern. For this reason, the EA pattern is often interpreted as a "southward shifted" NAO pattern. In this case, Figure IV-1 shows a configuration of a north-south anomaly centres dipole spanning the North Atlantic from west to east, displaying a configuration of positive and negative correlation values centred over the North Atlantic area. Maxima of latitudinal western/eastern wind mainly affect to the Iberian, Britain and French zones. Thus, such dynamically coherent configuration results in intrusions of maritime air masses over Iberia as it can be noted in the strong isotherm gradient in Figure IV-1.

Fourth mode

Figure IV-1, associated with the fourth mode, showss a col (Bluestein, 1992), maintaining the Iberian Peninsula in the intersection zone between the cyclonic and anticyclonic nuclei. The col (common in the "horse latitudes") is the intersecting zone between an anticyclonic axis (joining two high pressure centres facing each other) and a cyclonic axis (joining two low pressure centres facing each other). A col is characterised by substantial deformation in their vicinity and consequently is highly related to frontogénesis and frontolisis. Valero et al. (1997) have shown that these large-scale physical and dynamical configurations are related to extreme rainfall episodes in the Western Mediterranean. Such atmospheric configuration promotes northern (southern) air advection over the northern (southern) Iberia, leaving the remainder areas of Europe under the influence of low positive correlation values.

Fifth mode

This mode presents a spatial pattern (Figure IV-1) with longitudinally extended isolines in front of and covering the Iberian zone. With this configuration, low speed winds are expected over central Europe while, over Iberia and France, probability of high speed wind are supposed.

Sixth mode

This situation (Figure IV-1) seems to be associated with a omega blocking situation (Bluestein, 1992). In the region of the block, the weather remains essentially unchanged, as any transient weather disturbances are forced to circumvent the block. Once established, major blocking situations tend to persist for at least a week and appear to represent some quasi-equilibrium state of the atmosphere. In this sixth pattern, western European areas are affected by negative correlation values while the western and eastern areas are involved in positive value region. In the transition areas, high speed winds are expected.

Seventh mode

This SLP mode shows isolines correlation configuration similar to the fourth pattern (Figure IV-1), i.e., the spatial pattern displays a col. In this configuration the Iberian Peninsula is affected by high negative correlation values while most of Europe is under the influence of the col. As it is already mentioned, if at upper level cold air masses are juxtaposed over the col, instability on surface over such area is very intense, leading to strong precipitation and speed wind and decreased temperature.

Eight mode

The eight mode (Figure IV-1) shows over most of Europe very low correlation values, indicating low speed winds over the area. The meridional European zones, particularly the Mediterranean area, show negative/positive correlations, this configuration being representative of high speed wind in the transition areas.

Ninth mode

This mode (Figure IV-1) accounts for very low percentage variance. The spatial pattern shows low negative correlation values over Eastern Europe, highlighting areas with no significant isolines, being representative of low speed wind over Europe.

Tenth mode

The last significant mode of SLP (Figure IV-1) presents over Europe a positive and weak correlation centre over the east European areas, while western Europe is under a negative correlation centre. Such isolines configuration promotes advection of air masses over Iberia and eastern Mediterranean areas and weak advection over central Europe.

Chapter 5

Relationships between wind speed and large-scale atmospheric circulation

In this chapter, the relationships between wind speed and the large-scale atmospheric variables are explained for the Iberian window because the wind speed data field are only available for the Iberian Peninsula at this point. To examine the real circulation features associated with the wind patterns, a set of positive and negative composite plots are constructed from the dates with the 5% highest and lowest scores of the time series obtained of the PCA. Composites are defined here as the ensemble average of a set of synoptic maps of a large-scale atmospheric variable. The distinctive features in the composite plots take into account the physical realism as opposed to the statistical meaning of the derived spatial modes. Moreover, to show circulation features in the European window, although wind data are not available at this moment, some composite plots are also built.

The composite plots have been made from two points of view. First, the composites of large-scale atmospheric variables have been built for those weather configurations associated with the highest and lowest PCA scores of the wind speed. Thus, the composites represent the atmospheric state associated with particular wind characteristics.

Additionally, relationships between the composites and local wind speed are also provided. Thus, plots with probability values associated with the highest and lowest scores of the Z1000 PC time series are described.

5.1. Composites of large-scale variables conditioned by the wind speed. Iberian window.

In the previous chapters, the results of the PCA applied to large-scale and regional fields have been described. As it is abovementioned in the Introduction, in this chapter a set of real maps selected from the PCA time series are illustrated to show the atmospheric state. While the derived PC modes are statistically built, the composite maps represent configurations of the variable which are comparable to observations. So, similar to the relationship between observational patterns and the PC modes, positive (negative) composites are constructed directly from a number of configurations with high (low) time series values because they indicate situations in which the corresponding PC mode is dominant in its positive (negative) phase. The selected number of configurations represents 5% of the total number of cases in the dataset (Figure V-1).

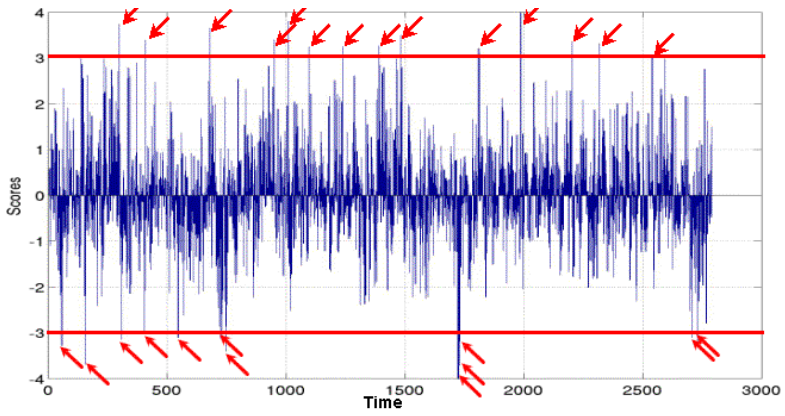

Figure V-1. Example of picked up dates from the PC time series. The red rows indicate the 5% high positive and negative scores used to built the composite maps.

The composite maps for the first ten modes of Z1000 for winter, described in Chapter 3, are depicted in Figures V-2 and V-3. This Figure shows the positive and negative composite plots of Z1000 conditioned to the top 5% PC scores of the wind speed (see Figure III-8). Subsequently, mean maps of Z1000, from these dates are built, highlighting the mean atmospheric state conditioned to predominant oscillation of the selected PC mode.

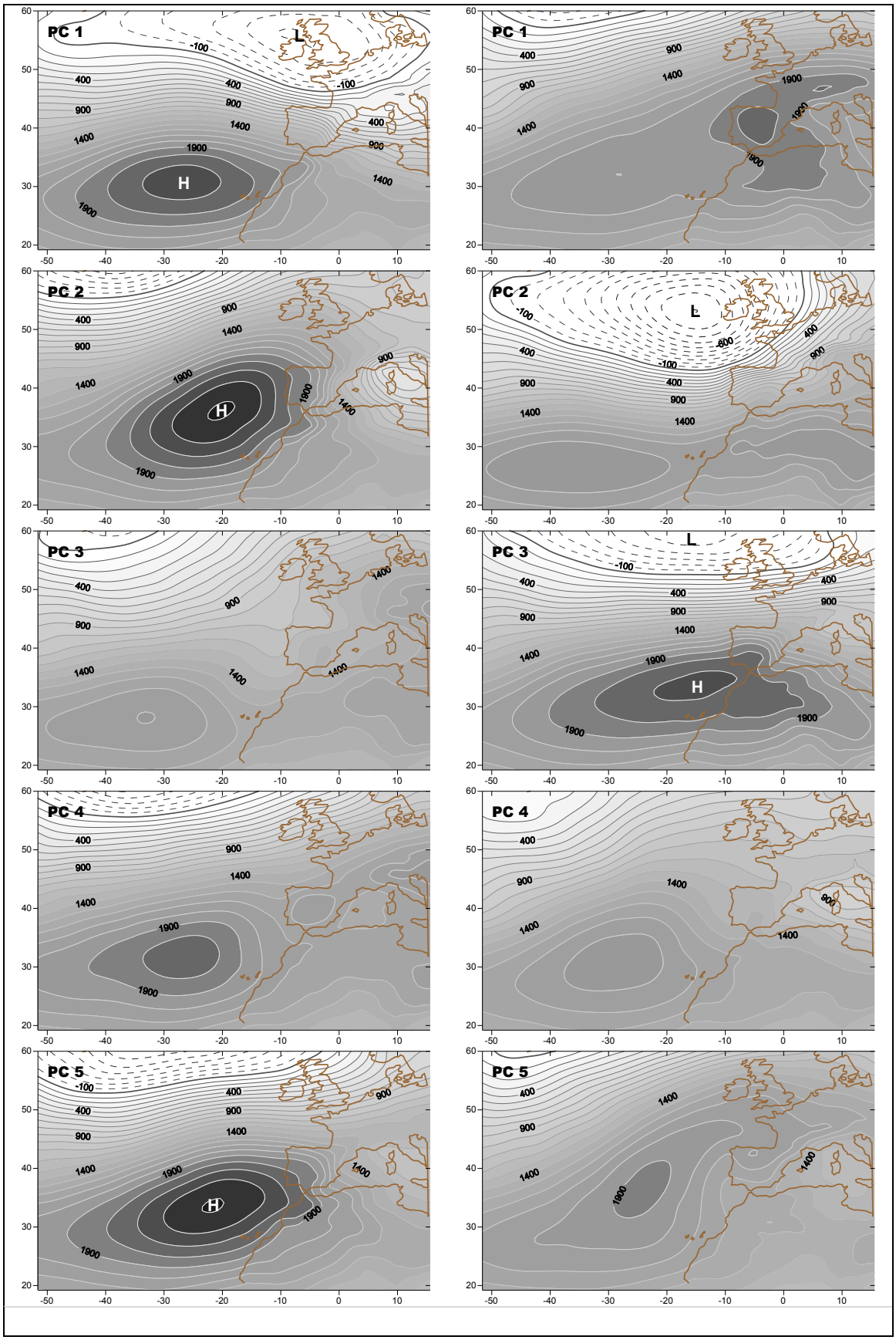

Figure V-2. Positive (left) and negative (right) composite plots of Z1000 selected by the 5% highest and lowest values of the PC time series of the observational wind speed for winter. This figure contains composites conditioned by wind field from the PC1 to PC5.

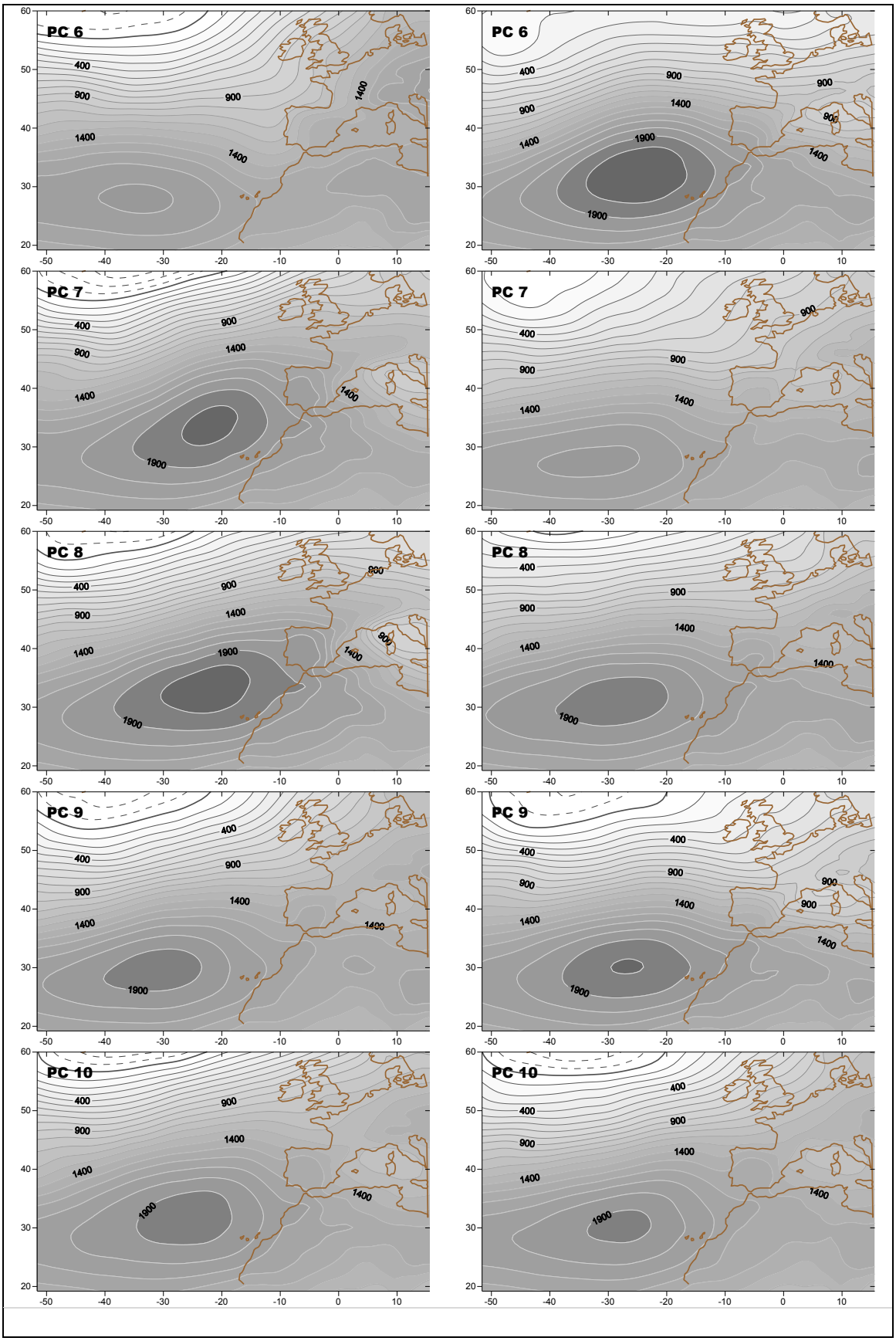

Figure V-3. Positive (left) and negative (right) composite plots of Z1000 selected by the 5% highest and lowest values of the PC time series of the observational wind speed for winter. This figure contains composites conditioned by wind field from the PC6 to PC10.

For sake of simplicity, only the most relevant results of winter will be explained. The Z1000 composites associated to the first wind PC (Figure V-2, first left and right panels) highlight two different mean atmospheric situations associated with the wind behaviour. Thus, in the first positive composite (left panel), a strong gradient of Z1000 is observed over the Iberian Peninsula, underlying strong winds over all Iberia. In contrast to this atmospheric situation, the first negative composite (right panel) displays high pressure over Iberia with little gradient, showing a nucleus over inner Iberia. This situation is indicative of either low wind speed over most of the area or different wind behaviour over Iberia (see Figure III-7).

The Z1000 composites associated to the second wind PC (Figure V-2, second left and right panels) also highlight two different atmospheric situations associated with the wind behaviour. Thus, in the second positive composite (left panel) it can be noted a Z1000 gradient over the Iberian Peninsula, promoting northwestern and north winds over Iberia (see Figure III-7). In the other hand, the second negative composite (right panel) reflects a dipolar configuration with a low located at western Britain and high pressures situated over the southern part of the study region, being the Iberian Peninsula in a very strong gradient area. This configuration promotes very strong eastwards winds blowing the Peninsula.

As an additional example, the Z1000 composites associated to the fifth wind speed PC (Figure V-2, fifth left and right panels) also highlights two different atmospheric situations. The fifth positive composite (left panel) shows a nucleus of high Z1000 values situated southwest of Iberia, promoting air mass advection over the south of Iberia. This atmospheric configuration produces south and southeastern winds over southern areas of Iberia, as shown in the PC5 of Figure III-7, with north-south differences in the wind behaviour over Iberia and high winds in the Gibraltar Strait.

In order to facilitate studies about these composites, dates used to build the composites are provided in the tables of Appendix II. In these tables, only the 1% of dates associated with the highest and lowest scores is supplied.

5.3. Composites of wind speed conditioned by the large-scale variables. Iberian window.

A set of mean observational maps selected from the PCA time series are shown to give a general picture about the wind behaviour. In order to show the relationship between observational patterns and the PC modes, positive (negative) wind composites are constructed directly from a number of dates with high (low) PC scores of Z1000 (Figure V-1).

The composite maps for the first ten modes of wind speed for winter, introduced in Chapter 3, are depicted in Figures V-4 and V-5. This Figure shows the positive and negative composite plots of wind speed conditioned to the 5% high PC scores of the Z1000 field (see Figure III-4). Subsequently, mean maps of wind speed are built.

The composites associated to the first Z1000 PC (Figure V-4, first left and right panels) highlight two different situations relative to the wind behaviour. In the first positive composite (left panel), similar wind behaviour is observed over Iberia, underlying a nucleus of strong winds located east to Gibraltar Strait. This situation is associated with the PC1 of Z1000 (Figure III-1), where the geopotential pattern was characterised by a north-south dipole configuration with one of the two centres located centred over the Canary Islands and another one situated east of Greenland. This situation promotes in its positive phase similar behaviour of the wind field over Iberia. The first negative composite (right panel) of Figure V-4 displays a configuration with similar isotachs throughout Iberia, highlighting some nuclei of strong wind speed in particular points. Thus, it is remarkable the presence of a nucleus of strong wind located at western Gibraltar Strait, according to the negative phase of the Z1000 PC1, displayed in Figure III-1.

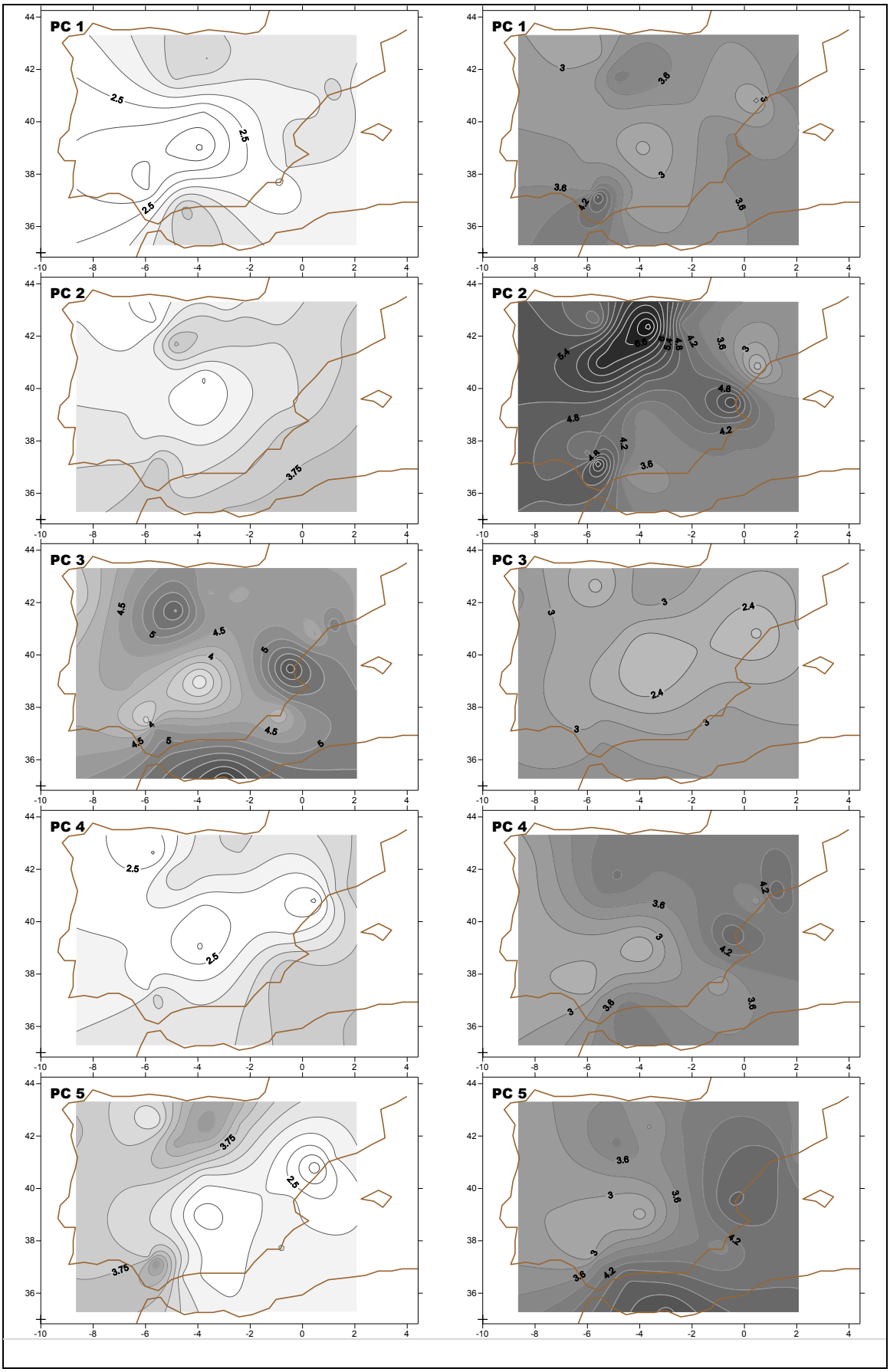

Figure V-4. Positive (left) and negative (right) composite plots of wind speed selected by the 5% highest and lowest values of the PC time series of the observational wind speed for winter. This figure contains composites conditioned by wind field from the PC1 to PC5.

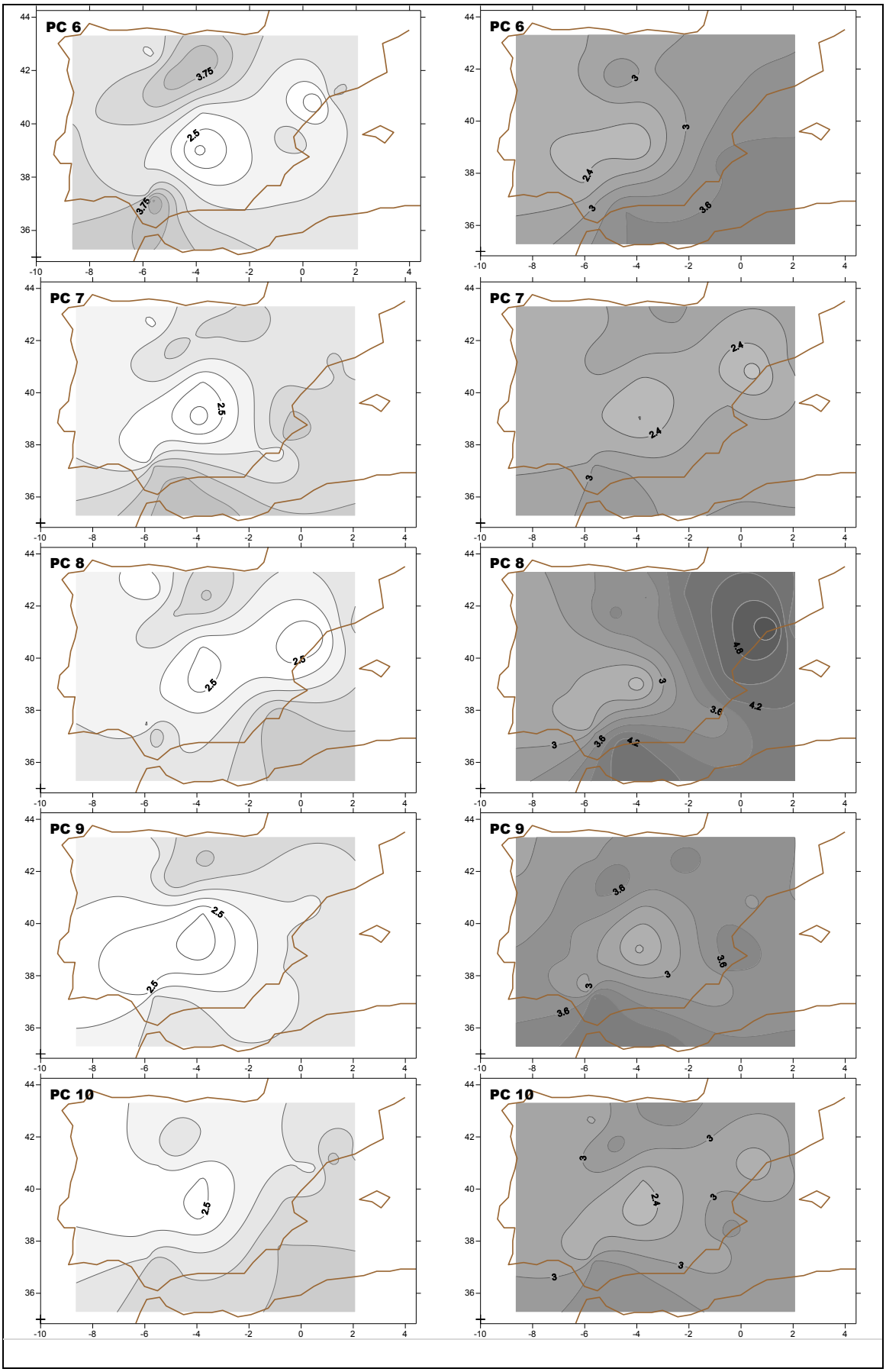

Figure V-5. Positive (left) and negative (right) composite plots of wind speed selected by the 5% highest and lowest values of the PC time series of the observational wind speed for winter. This figure contains composites conditioned by wind field from the PC6 to PC10.

The composites associated to the second Z1000 PC (Figure V-4, second left and right panels) indicate, in the first positive composite (left panel), a wind gradient over the Iberian Peninsula with strong winds over most of eastern Iberia. This situation is related with the positive phase of Z1000 in Figure III-1, where it can be noted a gradient of correlation isolines that promotes westward wind over the Mediterranean zones of the Peninsula. The second negative composite (right panel) is related to the negative phase of the Z1000 PC2 of Figure III-1, in which low pressures are located northwestern Iberia, and reflects strong wind speeds over most of Iberia, marking several nuclei of very strong winds: Ebro Valley, Catalonia and Gibraltar areas.

The remainder panels reflect diverse characteristics of the wind behaviour over Iberia. In analogous way to the previous section, in the tables of Appendix II only the 1% of dates associated with the highest and lowest scores is supplied.

5.4. Composites of mean sea level pressure in the European window.

Several composite maps related to the results of the PCA applied to mean sea level pressure are described in this section. Although wind data are not available at this moment for the European area, composite plots are also built in order to show real circulation features in the European window.

These composites have been built in analogous way to the described composites in previous sections. Thus, in order to indicate relationships between observational patterns and the PC modes, positive (negative) composites are constructed directly from a number of dates with the high (low) time series values as they indicate situations in which the corresponding PC mode is dominant in its positive (negative) phase. As there is no wind dataset in the European window, these SLP composite are not conditioned. The composites represent the highest 5% of the total number of cases in the dataset (Figure V-1).

The composites associated to the first SLP PC (Figure V-6, first left and right panels) highlight two different mean atmospheric situations. In the first positive composite (left panel), a low pressure area is covering most of Europe, showing no gradient over the area. On the contrary, the first negative composite (right panel) highlights a strong gradient of SLP over north-south Europe. Under this situation strong winds can be noticed over Europe, most probably over the Britain Islands, Scandinavian Peninsula and northern Europe in general.

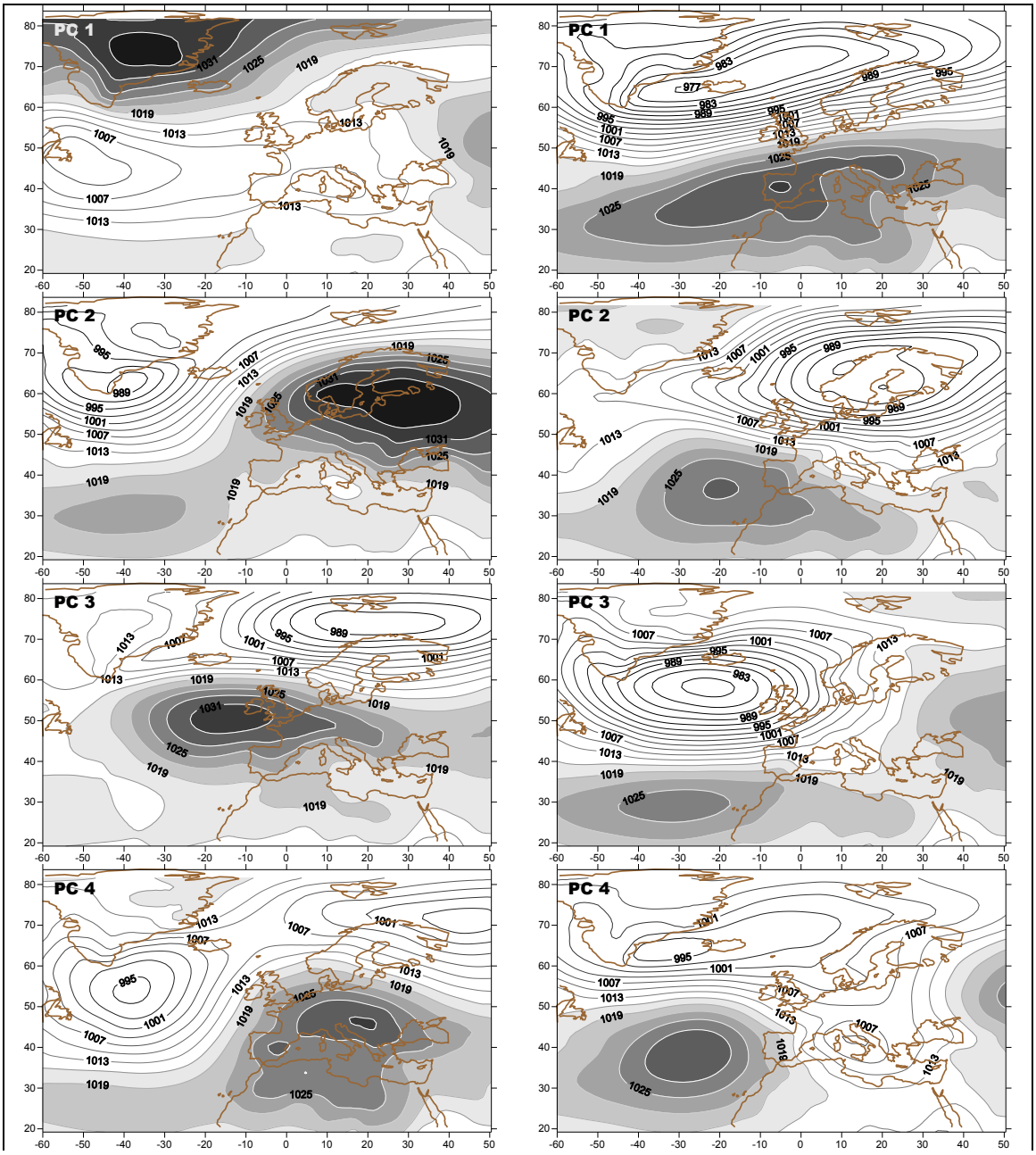

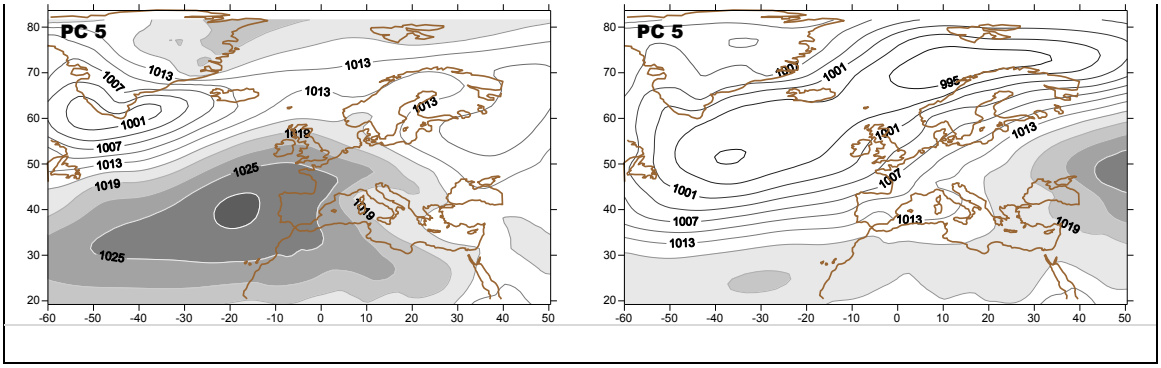

Figure V-6. Positive (left) and negative (right) composite plots of SLP selected by the 5% highest and lowest values of its PC time series. This figure contains composites from the PC1 to PC5. Shadow areas correspond to high pressure zones.

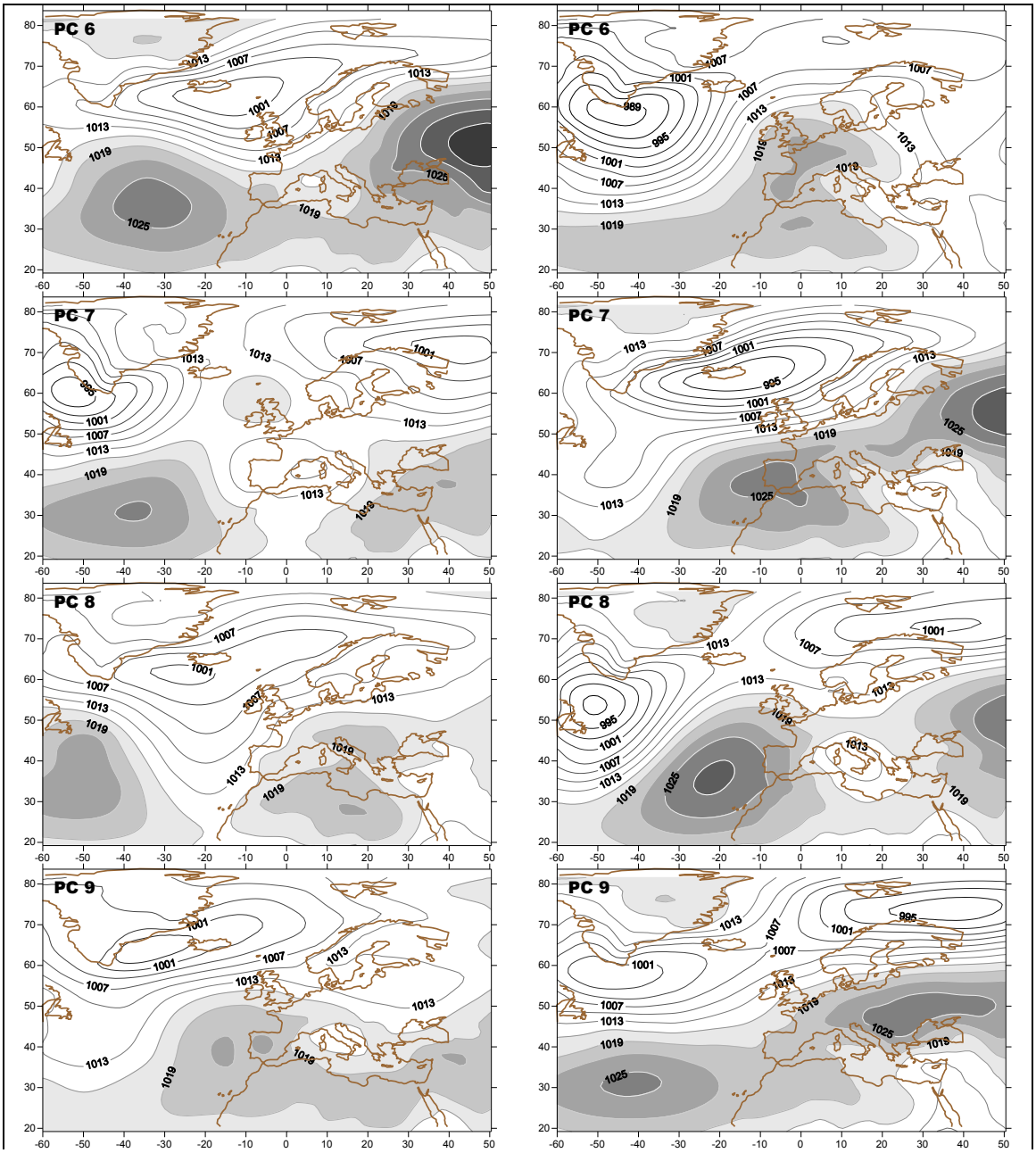

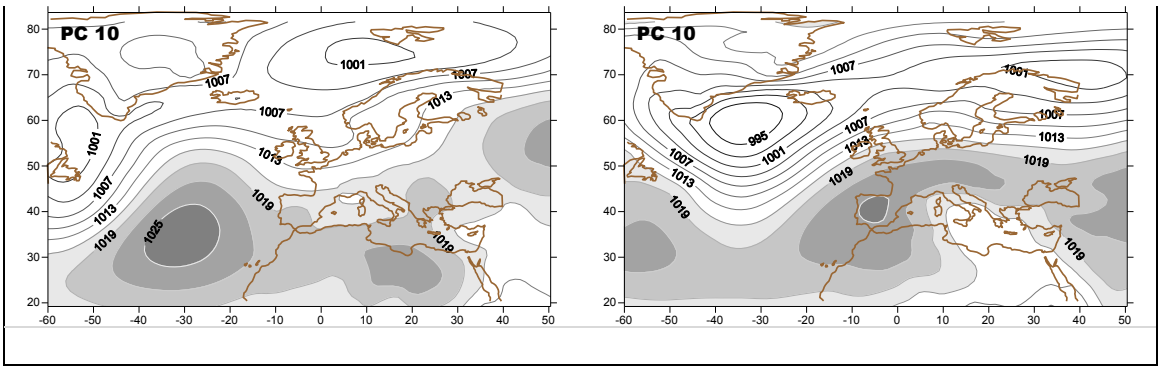

Figure V-7. Positive (left) and negative (right) composite plots of SLP selected by the 5% highest and lowest values of its PC time series. This figure contains composites from the PC6 to PC10. Shadow areas correspond to high pressure zones.

The composites associated to the second SLP PC (Figure V-6, second left and right panels) show, in the first positive composite (left panel), a high pressure zone over inner Europe, while low pressures are located at northwestern area of study. This situation drives strong winds around the Britain Islands (see Figure IV-1). In the other hand, the second negative composite (right panel) reflects a dipolar configuration with a low located over the Scandinavian Peninsula and high pressures situated over the southwestern part of the study region, most of Europe being in a very strong gradient area. This configuration fosters very strong winds blowing from the Russian areas to inner Europe.

As an additional example, the positive composite associated to the seventh SLP PC (Figure V-7, fifth left panel) show most of Europe without pressure gradients. The negative composite displays a northwestern-southeastern isobar configuration, leaving the Britain Islands, the Scandinavian areas, Denmark and northern France under influence of a low pressure nucleus, promoting maritime air mass advection over these areas. This atmospheric configuration produces western winds as observed in the PC7 of Figure IV-1.

Dates used to build the composites are provided in the tables of Appendix II. In these tables, only the 1% of dates associated with the highest and lowest scores is supplied.

5.5. Cumulated Probabilities of wind speed associated with the large-scale variables.

This section attempts to show the relationships between the obtained PCs and the observational wind speed in several stations described in Chapter 2. To this end, the cumulated frequency of wind speed associated to the different PC is obtained. These plots will give a fair idea about the observational wind frequency distributions conditioned to the different dominant scores of the PC time series.

Figures V-8a and 8b show the wind speed cumulated frequencies for several stations associated to dominant positive scores of the PCs of Z1000. To do this, as it is abovementioned the high Z1000 scores are selected, associated with their dates. At every station, the wind speed is picked up for such dates, depicting the associated cumulative probabilities from 0 to 100%.

In general, it is remarkable the high frequency of the Z1000 PC3 at wind speeds. The third PC (Figure III-1) showed a configuration of positive (negative) correlation values centred over the North Atlantic area (Western Europe) with light northeastern-southwestern orientation. Maxima of latitudinal western wind mainly affect to the northern zones of Europe, Russian and the Scandinavian Peninsula while the meridional flows are maxima in the western North Atlantic area over Iceland and northern flows can be noticed in the vicinity of Iberia. Thus, such configuration result dynamically coherent, and is characterized by intrusions of air masses over Iberia as it can be noted in the high wind values in Figures V-8a and b. This Z1000 PC has the strongest influence over the observational wind speeds in all Iberia, with wind speeds up to $10ms^{-1}$ in most of the stations, reaching $14ms^{-1}$ in Valencia.

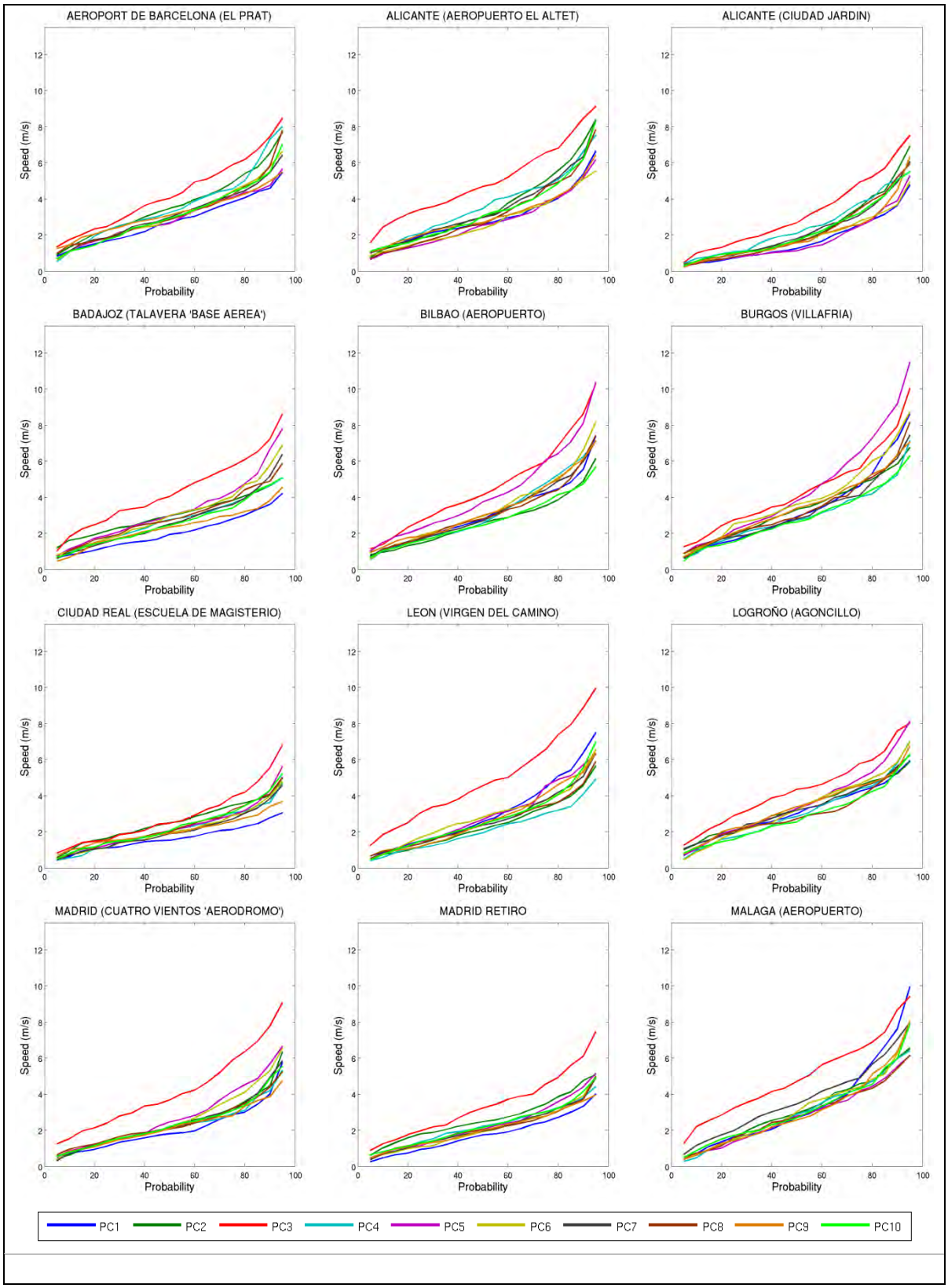

Figure V-8. (a) Wind speed cumulated frequencies associated to the strong positive scores of Z1000 PCs for several stations.

Besides PC3, PC5 is also predominant in high wind situations. For example, in Bilbao, Burgos, Morón de la Frontera and Zamora stations, the presence of PC5 is comparable to PC3 with observational wind speed reaching 12ms^{-1}. This fifth mode presented a spatial pattern very similar to the third mode except for the centre of negative anomalies locate in between two strong nuclei of positive anomalies (Figure III-1). The isolines are longitudinally extended which represents strong northern (southern) air advection over Iberia.

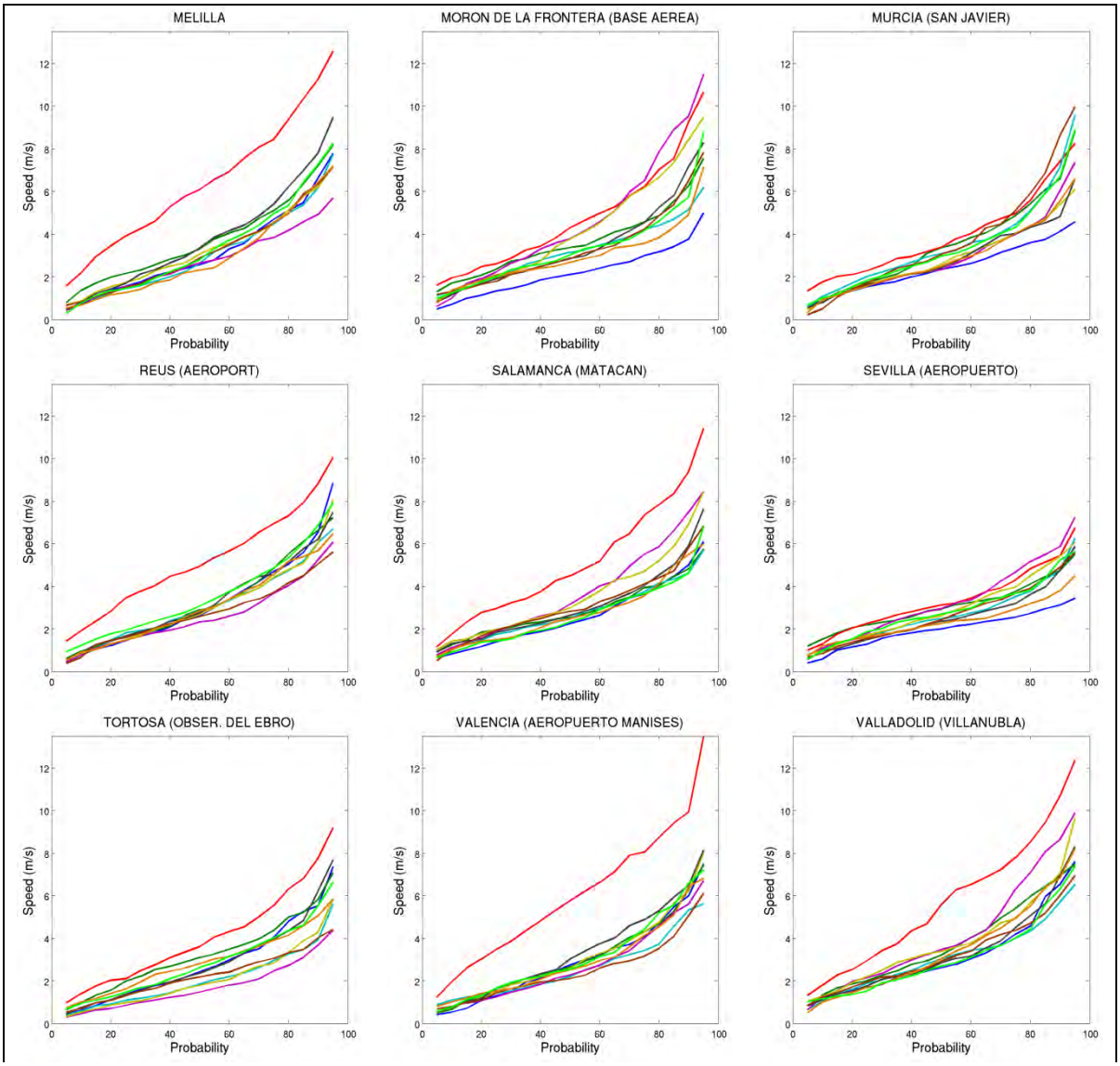

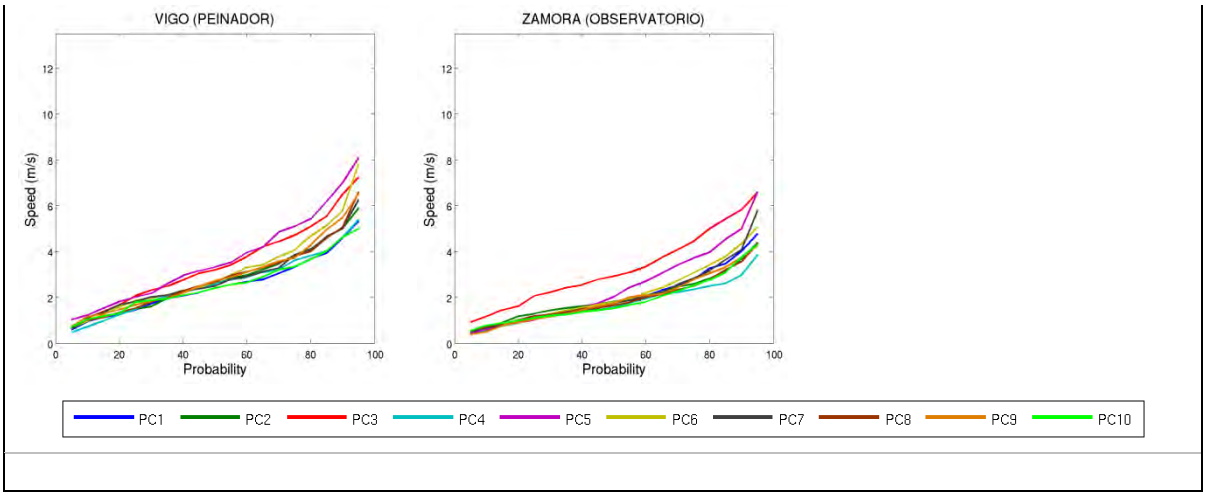

Figure V-8. (b) Wind speed cumulated frequencies associated to the strong positive scores of Z1000 PCs for several stations.

Similar to the Figures V-8, Figures V-9a and 9b show the wind speed cumulated frequencies for several stations associated to the strong negative scores of the PCs of Z1000. In this case, the high negative Z1000 scores are selected and at every station, the wind speed is picked up for such dates, to depict the associated cumulative probabilities from 0 to 100%.

This time the dominant PC over the wind speed in all stations is the PC2, which shows strong dipolar structure with a centre of high positive anomalies over the North Atlantic Ocean and negative anomalies, located over the southern area of study. Thus, such configuration is characterized by intrusions of westerns/eastern air masses over Iberia. This pattern has strong influence over the observational wind speed in all Iberia, with extreme wind speeds of around 12ms^{-1} in Morón de la Frontera.

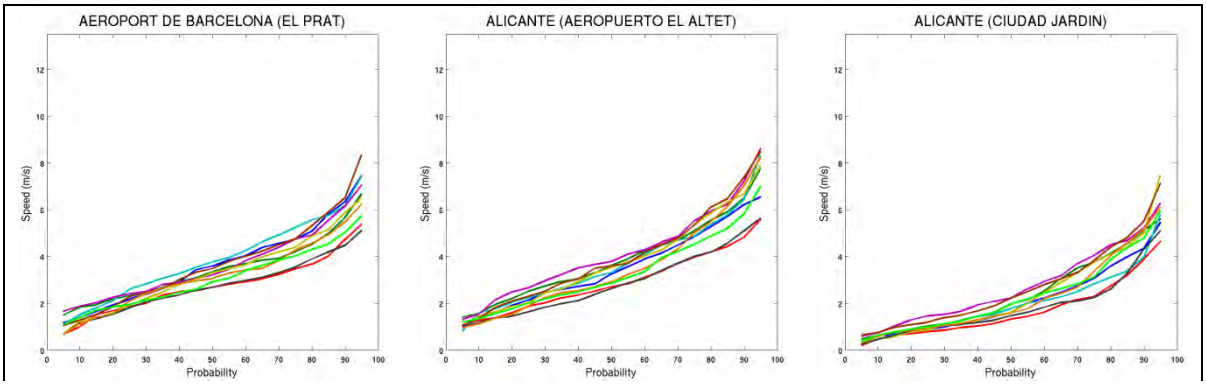

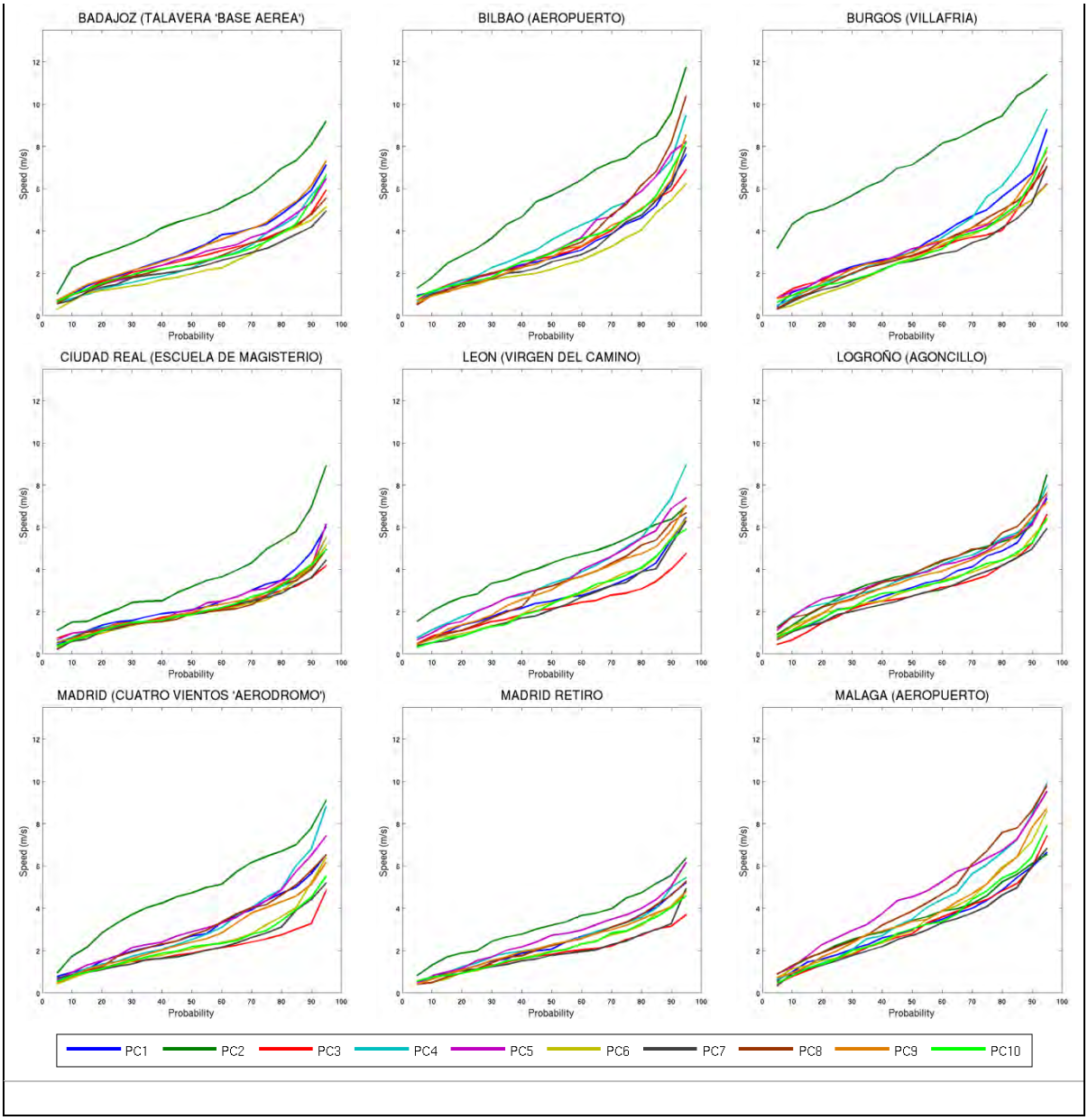

Figure V-9. (a) Wind speed cumulated frequencies associated to the strong negative scores of Z1000 PCs for several stations.

It is also remarkable the influence of PC8 in Reus and Tortosa stations with wind speed values higher than 10 ms^{-1}. The eight mode (Figure III-1) shows low negative correlation values over Iberia in between two zones of positive correlations. This configuration promotes meridionally air mass advection over Iberia with decrease or increase temperature depending on the air direction.

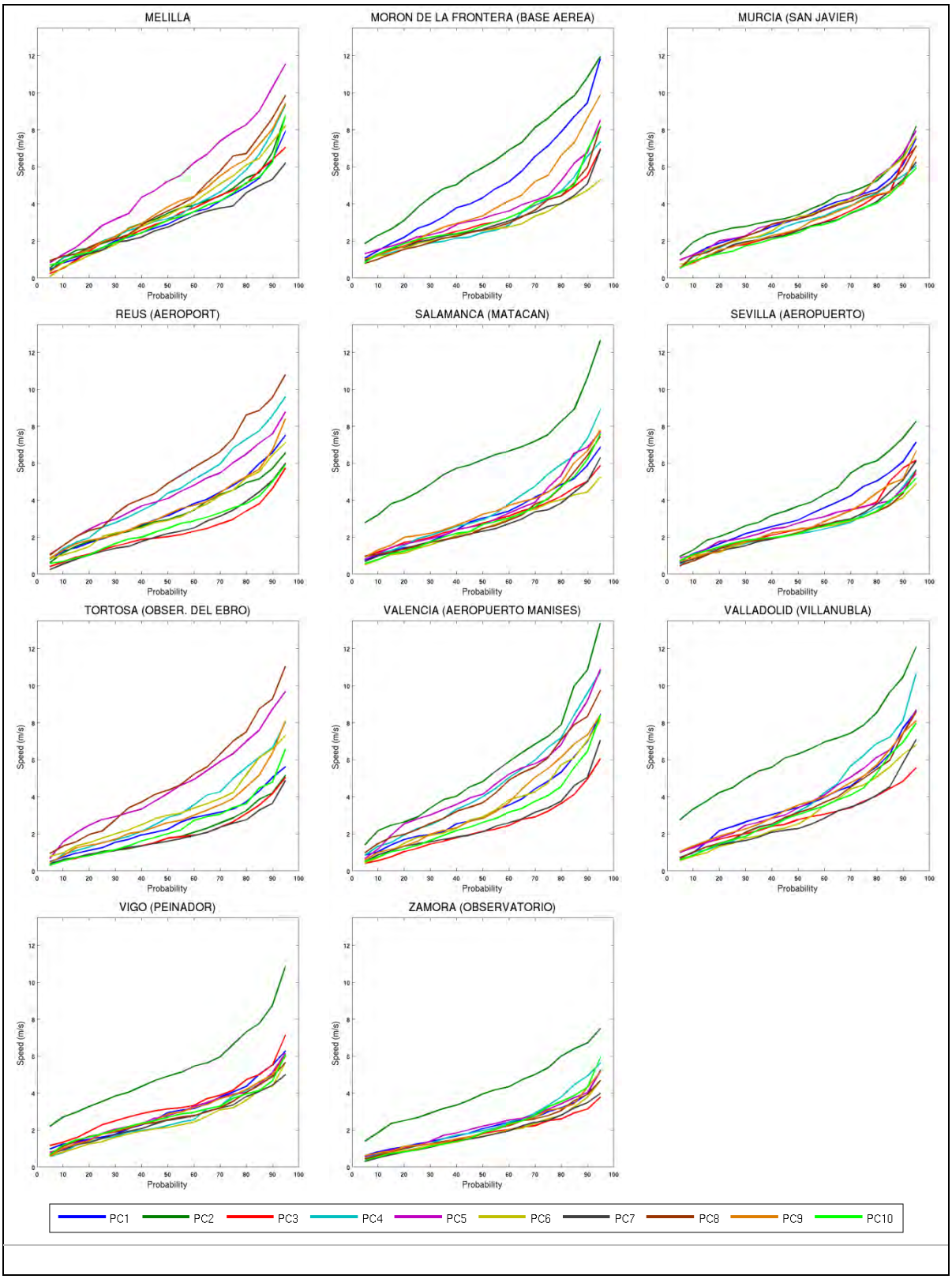

Figure V-9. (b) Wind speed cumulated frequencies associated to the strong negative scores of Z1000 PCs for several stations.

Chapter 6

Conclusions

In the framework of the *SafeWind* project, the UCM partner has developed an objective classification of the Atlantic large-scale atmospheric situations, establishing relationships between significant synoptic atmospheric situations and wind speed. A weather pattern classification is shown by means of a multivariante methodology, also explaining each obtained significant mode in terms of different teleconnection patterns and/or other atmospheric features. The purpose of this deliverable is to show the different work phases and the main obtained results.

The deliverable has been built in several chapters. In Chapter 1, a brief introduction explains the main objectives of the work. Chapter 2 shows the different data bases as well as the methodology used in the deliverable. Thus, several sets of variables have been used: large-scale variable sets and regional variable. The large-scale database used in this study consisted of daily means of several variables over a grid of 1.2º x 1.2º (lat x lon) resolution for the period 1971-2007. The variables are extracted from the global data base ERA40 from the European Center Medium Weather Forecast (ECMWF) (Uppala et al., 2005). In a first step, an Iberian window is used with a selected domain that spans the North Atlantic Ocean, the Mediterranean Sea and part of Europe, covering from 20º N to 60º N of latitude and from 51.5º W to 15.5º E of longitude. The regional variable

consisted of the 6-h wind data. From these data, time series of daily and monthly mean wind speed were also built for 23 stations covering the 1980-2001 period. All the time series have had a quality control process. All data bases were seasonally grouped: Winter (DJF), Spring (MAM), Summer (JJA) and Autumn (SON). In order to cover all the *SafeWind* test cases, a second step was done. An European window is used with a large-scale spatial domain that spans the North Atlantic Ocean, the Mediterranean Sea and Europe from 20º N to 85º N latitude and from 60º W to 50º E longitude. Here, the large-scale data base used in this study consists of daily means data of sea level pressure over a grid of 2.5º x 2.5º (lat x lon) resolution for the period 1958-2007, selected also from the global data base ERA40.

The methodology used in this work has been a multivariante technique: the principal component analysis. The principal component analysis (PCA) was applied to the large-scale atmospheric circulation and the wind databases in the case of the Iberian window and for the European window it was applied to the large-scale variable. The PCA has proven to be a reliable method for data reduction and for examining the variance structure. An appendix is also provided to present more details about this multivariante technique.

In Chapter 3, the results obtained of applying the PCA to the different wintertime and springtime datasets were shown. Thus, from the obtained modes, spatial patterns, accounting for more variance of the original data, of geopotential, temperature and relative humidity, are shown for the Iberian window and for wintertime and springtime. The most significant spatial patterns were explained in terms of their relationships with several low-frequency Atlantic teleconnection patterns (NAO, EU, etc) and other characteristics (omega blocking configuration, col pattern, etc). The analysis in the temporal domain was made by means of continuous wavelet analysis, providing several features of the PC time series. The variable regional has been also explained, showing the most important types of wind blowing the Iberian Peninsula as well as the most significant principal components (see the flow diagram). In order to extend the study to the rest of Europe, the whole analysis was applied to the spatial window covering the European domain. Similar spatial patterns are obtained and again are explained in terms of

teleconnection patterns and other features. Chapter 4 shows the results obtained of applying the methodology to the dataset of the European window. Thus, the most significant spatial and temporal patterns of sea level pressure are shown for this new window.

In order to examine both the spatial configuration of the wind field and the estimate values of the Iberian winds associated with the different statistical pattern obtained from the PCA, Chapter 5 presents the relationships, for the Iberian window, between the wind speed field and the large-scale atmospheric patterns used in this deliverable. Thus, the circulation features associated with the wind patterns were examined by means of composite maps. A set of positive and negative composite plots were obtained from the dates with the 5 and 95 percentiles of the scores of the time series obtained of the PCA (see the flow diagram). Composites were defined as the ensemble average of a set of synoptic maps of a large-scale atmospheric variable. The distinctive features in the composite plots take into account the physical realism as opposed to the statistical meaning of the derived spatial modes. Dates used to build the composites are provided in the tables of Appendix II. The composites associated to the first PCs highlight different situations relative to the wind behavior. Depending on the spatial PC pattern, both in the positive and negative composites, differences in the wind behavior over Iberia are shown, also underlying nucleus of strong winds over particular areas. Thus, the composites associated to the first geopotential height PC (the most significant statistical mode) highlight two different situations relative to the wind behavior. In the first positive composite, similar wind behavior is observed over Iberia, underlying a nucleus of strong winds located east to Gibraltar Strait. This situation is associated with the PC1 of the geopotential height, where the geopotential pattern was characterized by a north-south dipole configuration with one of the two centers located centered over the Canary Islands and another one situated east of Greenland. This situation promotes in its positive phase similar behavior of the wind field over Iberia. On the other hand, the first negative composite showed a configuration with similar isotachs throughout Iberia, highlighting some nuclei of strong wind speed in particular points. Thus, there is the link between the obtained large-scale spatial configuration with the wind field, since it was remarkable the

presence of a nucleus of strong wind located at western Gibraltar Strait, according to the negative phase of the first PC of the geopotential height.

Additionally, in order to show relationships between the obtained PCs and the observational wind speed in several stations described in Chapter 2, wind speed cumulated frequencies associated to the different PCs are also obtained and shown in Chapter 5. The frequency plots will give an idea about the observational wind frequency distributions conditioned to the different dominant scores of the PC time series (see the flow diagram). To do this, as it is abovementioned the high scores of the 9 and 95 percentiles are selected and associated with their dates and at every station, the wind speed is picked up, depicting the associated cumulative probabilities from 0 to 100%. The third PC of the geopotential height shows the strongest influence over the observational wind speeds in all Iberia in the positive phase, with wind speeds up to $10ms^{-1}$ in most of the stations, reaching $14ms^{-1}$ in the eastern peninsula. On the other hand, the wind speed cumulated frequencies for several stations associated to the strong negative scores of the PCs are also shown. The dominant PC over the wind speed in all stations is the PC2, which showed strong dipolar structure with a centre of high positive anomalies over the North Atlantic Ocean and negative anomalies located over the southern area of study. Such configuration promoted intrusions of westerns/eastern air masses over Iberia. This pattern presents strong influence over the observational wind speed in all Iberia, with extreme daily mean wind speeds of around $12ms^{-1}$ in the southern area.

In summary, different types of large scale atmospheric circulation patterns were obtained by means of principal components analysis, showing a weather classification over the Atlantic area. The relationships between some circulation patterns and the wind field in different stations of the Iberian Peninsula have been well highlighted. The dates corresponding to each of the weather types found are supplied, allowing finding some particular situations. Interesting links about the relationships between the wind field and the large scale atmospheric structures are found.

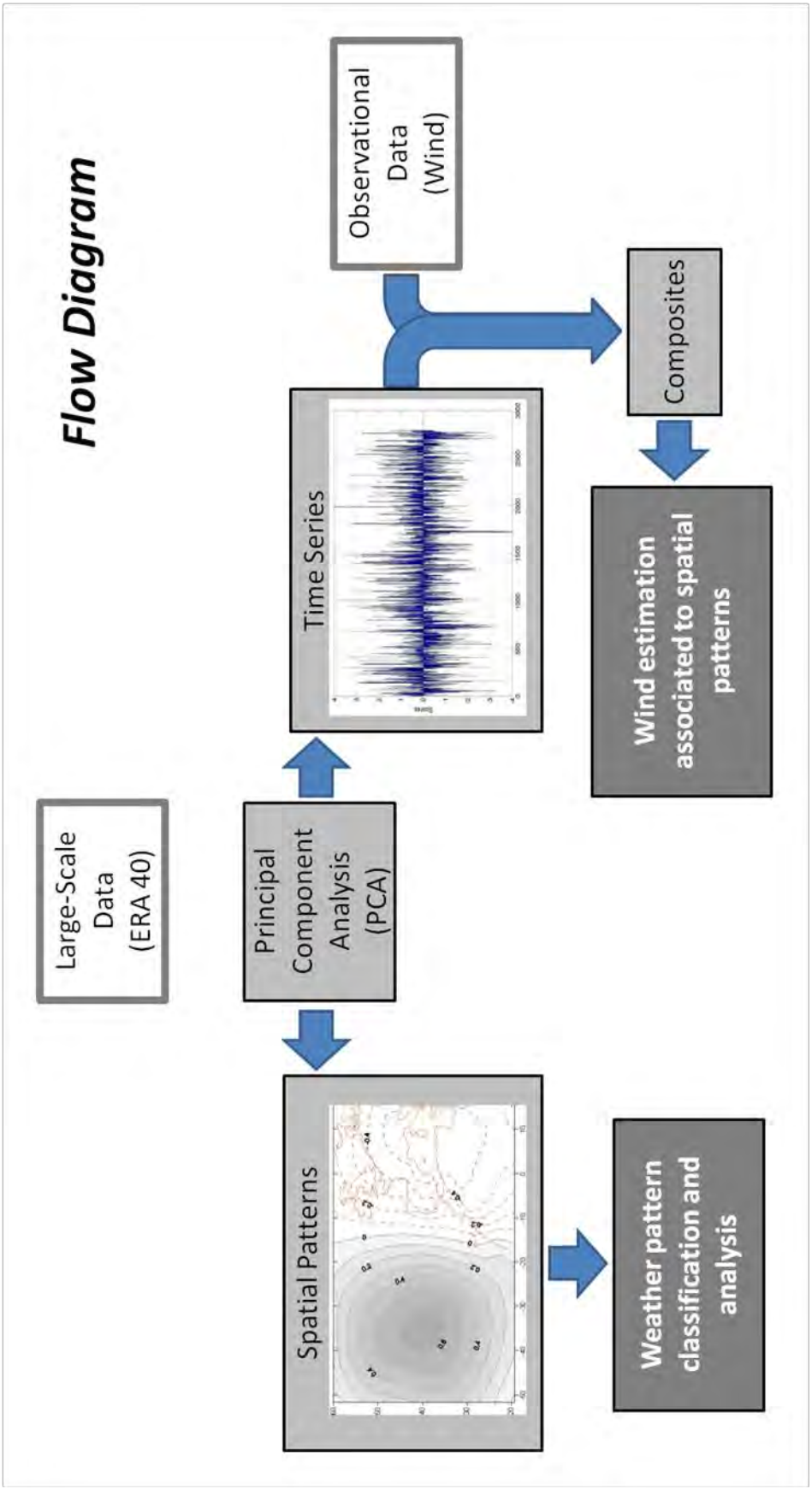
Flow Diagram
Large-Scale Data (ERA 40)
Principal Component Analysis (PCA)
Spatial Patterns
Weather pattern classification and analysis
Time Series
Observational Data (Wind)
Composites
Wind estimation associated to spatial patterns

Appendix I

Principal component analysis

In order to extract the general behaviour of a data set, principal component analysis (PCA) has been applied to the large-scale atmospheric circulation and the wind databases. The PCA has proven to be a reliable method for data reduction and for examining the variance structure (Preisendorfer 1988). This methodology applied to spatial data, known as S-mode decomposition (Richman 1988), enables patterns to be identified that can be attributed to specific physical processes by statistical assessment. The new uncorrelated variables are called principal components (PCs) and consist on linear combinations of the original variables derived from the diagonalization of the covariance/correlation matrix. The coefficients of the linear combinations represent the weight of the original variables in the PCs and they are named *loadings* or PC patterns. The PCs indicate modes of variation of the original field and are numbered according with their related variance. Thus, the first PC is the linear combination with the maximum possible variance, the second one is the linear combination with the maximum possible variance which is uncorrelated with the first PC and so on (Jolliffe, 1986; Sneyers et al. 1989) . The projection of the original series onto each eigenvector gives as result the time-dependence coefficient named *scores* or PC time series.

In our case, the PCA was applied to the correlation matrices of both datasets, the large-scale variables and observed wind fields and a set of eigenvalues and

eigenvectors are produced. Generally, the most important (the first ones) eigenvectors tend to describe regions with largest fluctuations. Thus, most information from the data can be represented using some smaller number of the principal components and a much smaller data set. The PCA was described by Pearson and Hotelling and introduced in meteorology by Lorenz (Lorenz, 1956).

The PCA method is based on the theorem:

Let **X** be a m-dimensional matrix with mean μ and covariance matrix **S**. Let $\lambda_1 \geq \lambda_2 \geq \ldots \lambda_m$ be the eigenvalues of **S** and let $p_1,\ldots, p_m$ be the corresponding eigenvectors of unit length. The **S** matrix is *Hermitian*; thus, the eigenvalues are non-negative and the eigenvectors are orthogonal.

Characteristics of these matrices and vectors can be seen in a more clear way by the following *tableau*:

Let **X** (n x p) be a m-dimensional matrix of n independent observations and p ramdom elements:

$$\mathbf{X} = \begin{pmatrix} x_{11} & \ldots & x_{1p} \\ \ldots & \ldots & \ldots \\ x_{n1} & \ldots & x_{np} \end{pmatrix}$$

Where files correspond to observations and columns to variables. For sake of brevity, it is assumed μ**=0**.

Let **S** be the covariance matrix of **X,** obtained as:

$$\mathbf{S} = \left\langle \mathbf{X}^{\mathrm{T}}\mathbf{X} \right\rangle = \frac{1}{n-1}\begin{pmatrix} \sum_{i=1}^{n} x_{i1}x_{i1} & \ldots & \sum_{i=1}^{n} x_{i1}x_{ip} \\ \ldots. & \ldots. & \ldots \\ \sum_{i=1}^{n} x_{ip}x_{i1} & \ldots & \sum_{i=1}^{n} x_{ip}x_{ip} \end{pmatrix} = \begin{pmatrix} s_{11} & \ldots & s_{1p} \\ \ldots & \ldots & \ldots \\ s_{p1} & \ldots & s_{pp} \end{pmatrix}$$

Let **R** the correlation matrix of **X** obtained as:

$$\mathbf{R} = \begin{pmatrix} 1 & \dots & \frac{s_{1p}}{\sqrt{s_{11}s_{pp}}} \\ \dots & \dots & \dots \\ \frac{s_{p1}}{\sqrt{s_{11}s_{pp}}} & \dots & 1 \end{pmatrix} = (diag(\mathbf{S}))^{-1/2}\ \mathbf{S}\ \ (diag(\mathbf{S}))^{-1/2}$$

The **R** y **S** matrices are real, symmetric and semidefined positive. Thus, the matrix of a random variable **X** of dimension *p* and the purpose is to find a new variable, **A**, where:

$$\mathbf{A} = \mathbf{X}\,\mathbf{P}$$

The matriz **P** is chosen to maximize the sample variance of the new variable **A**:

$$\sum_{i=1,\, j=1}^{p,p} s_{ij} p_i p_j = \mathbf{P^T S P} \ \rightarrow \max$$

subject to:

$$\sum_{i=1}^{\mathrm{p}} p_i p_i = \mathbf{P^T P} = 1$$

This is equivalent to maximising:

$$P^T SP + \lambda(1 - P^T P) \ \rightarrow \ \max$$

The straightforward solution to this quadratic optimization problem is given by solving the eigenvalue problem:

$$\frac{d}{dP}(P^T SP + \lambda(1 - P^T P)) = SP - \lambda P = 0 \Leftrightarrow SP = \lambda P$$

where λ is the Lagrange multiplier associated with the constraint

$$\sum_{i=1}^{p} p_i p_i = \mathbf{P^T P} = 1$$

The PCAs are the eigenvectors of the sample covariance marix **S** arranged in decreasing order of the eigenvalues. The first eigenvalue gives the first principal component with the largest variance; the second eigenvalue gives the second principal component with the next largest variance subject to being orthogonal to the first eigenvector and so on.

PCA and eigenvalues

In order to find the principal components is summarized to find the eigenvalues, λ_i, and eigenvectors, p_i, of **S** arranged in decreasing order.

$$\mathbf{S} = \mathbf{P}\Lambda\mathbf{P}^T$$

where Λ is the diagonal (m x m) matrix composed of the eigenvalues of **S**.

Since the **S** (**R**) matriz is Hermitian all their eigenvalues are non-negative and their eigenvectors are orthogonal:

$$p_i^T p_i = \begin{cases} 0 & i \neq j \\ 1 & i = j \end{cases}$$

The a_i-s **principal components**, with variance λ_j equal to v*ar(p$_i$x$_j$)*. The first component accounts for the most proportion of variance associated with the original data. Each obtained component is associated with a **time series** of de *n* observations $a_j = \boldsymbol{p}_i^T \boldsymbol{X}$.

$$a_{ij} = \sum_{k=1}^{p} X_{ik} p_{kj}$$

These time series, a_j , are characterized by a null covariance value between them:

$$\mathrm{cov}(a_i, a_j) = 0 \qquad i \neq j$$

It therefore follows that:

$$\sum_{j=1}^{p} \lambda_j = \mathrm{tr}(\mathbf{\Lambda}) = \mathrm{tr}(\mathbf{S}) = \sum_{j=1}^{p} s_{jj}$$

The elements of the eigenvector $\boldsymbol{p}_j$ are the coefficients of the j-th principal component a_j.

The **Correlation** between the original data and the principal components are given by:

$$r\left[\mathbf{X_i}, \mathbf{a_j}\right] = \frac{\left\langle X_i, a_j \right\rangle}{\left\langle a_j^2 \right\rangle^{\frac{1}{2}}} = \frac{\left\langle a_i p_i, a_j \right\rangle}{\left\langle a_j^2 \right\rangle^{\frac{1}{2}}} = \frac{\left\langle a_j p_j, a_j \right\rangle}{\left\langle a_j^2 \right\rangle^{1/2}} = \left\langle a_j^2 \right\rangle^{1/2} p_j = \lambda_j^{1/2} p_j$$

The correlation between the original data **X** and the principal component a_j is equal to the eigenvector p_j multiplied by the root of the eigenvalue λ_j. Therefore, components of the p_j vector are proportional to the correlation between the original data and the principal component. Instead of the diagonalisation of the covariance matix, **S**, it is diserable some times the diagonalisation of the

correlation matrix, **R**, in such way that the sum of the eigenvalues is the dimension of the original variable, *p*.

The **variance** of the j-th component is λ_j. Usually, the component j-th accounts of the:

$$\frac{\lambda_j}{\sum_{j=1}^{p}\lambda_j} \text{ x 100 percentage of explained variance}$$

The most significant patterns are obtained from the first principal components. Their eigenvectors and the information of their time evolution, in terms of intensity and phase, are enclosed in the time series associated to each component.

Appendix II

Tables of dates related with composites

PC1	PC2	PC3	PC4	PC5	PC6	PC7	PC8	PC9	PC10
01-Dec-1976	20-Dec-1975	17-Jan-1972	18-Dec-1972	05-Feb-1972	16-Jan-1973	27-Feb-1972	27-Dec-1972	10-Dec-1971	11-Feb-1973
10-Dec-1982	21-Dec-1975	13-Feb-1973	19-Dec-1972	07-Feb-1973	18-Dec-1976	02-Feb-1976	19-Dec-1973	16-Dec-1973	18-Dec-1974
04-Jan-1983	24-Dec-1975	14-Feb-1973	06-Feb-1975	19-Dec-1973	22-Feb-1977	24-Feb-1979	23-Dec-1974	19-Dec-1974	31-Dec-1975
05-Jan-1983	07-Jan-1977	15-Feb-1973	04-Feb-1976	14-Jan-1975	09-Jan-1982	26-Dec-1979	30-Dec-1975	20-Dec-1974	03-Jan-1976
06-Jan-1983	25-Feb-1979	26-Jan-1976	05-Feb-1976	08-Dec-1976	11-Jan-1982	28-Jan-1981	31-Dec-1975	21-Dec-1974	20-Dec-1979
26-Jan-1983	26-Feb-1979	01-Feb-1976	12-Feb-1981	23-Dec-1977	18-Jan-1983	03-Dec-1982	23-Feb-1978	22-Dec-1974	11-Feb-1981
27-Jan-1983	12-Jan-1980	02-Dec-1976	13-Feb-1981	18-Jan-1979	19-Jan-1983	04-Dec-1982	20-Dec-1978	03-Jan-1976	02-Dec-1981
28-Jan-1983	28-Dec-1980	03-Dec-1976	04-Feb-1982	12-Feb-1981	07-Jan-1984	16-Jan-1985	09-Feb-1980	07-Jan-1976	17-Jan-1984
26-Feb-1983	08-Jan-1981	04-Dec-1976	20-Feb-1985	13-Feb-1981	08-Jan-1984	12-Feb-1985	28-Feb-1981	08-Jan-1976	29-Dec-1985
11-Jan-1986	09-Jan-1981	13-Jan-1981	28-Feb-1986	14-Feb-1981	15-Feb-1985	13-Feb-1985	22-Feb-1983	11-Jan-1976	23-Dec-1986
05-Jan-1989	10-Jan-1981	17-Dec-1982	26-Dec-1989	30-Dec-1981	16-Feb-1985	01-Jan-1986	28-Jan-1984	12-Jan-1976	28-Jan-1987
19-Feb-1989	11-Jan-1981	21-Dec-1982	27-Dec-1989	03-Feb-1982	17-Feb-1985	01-Feb-1987	16-Dec-1984	25-Feb-1976	19-Dec-1987
20-Feb-1989	03-Dec-1981	29-Jan-1986	28-Dec-1989	04-Feb-1982	26-Dec-1985	05-Dec-1990	17-Dec-1984	26-Feb-1976	16-Jan-1988
21-Feb-1989	04-Dec-1981	30-Jan-1986	30-Dec-1989	06-Feb-1982	15-Jan-1986	05-Feb-1991	17-Jan-1988	08-Jan-1977	17-Jan-1988
25-Jan-1990	10-Feb-1984	31-Jan-1986	31-Dec-1989	21-Jan-1985	20-Dec-1986	06-Feb-1991	19-Jan-1988	09-Jan-1977	30-Jan-1988
24-Feb-1990	13-Feb-1984	01-Feb-1986	25-Feb-1991	06-Jan-1992	21-Dec-1986	17-Dec-1992	20-Jan-1988	22-Feb-1979	14-Feb-1989
25-Feb-1990	25-Feb-1988	09-Feb-1988	28-Feb-1992	17-Jan-1995	12-Jan-1987	04-Jan-1993	14-Feb-1988	02-Dec-1980	26-Dec-1989
26-Feb-1990	26-Feb-1988	24-Feb-1989	26-Dec-1992	21-Jan-1996	13-Jan-1987	18-Feb-1994	02-Feb-1993	01-Jan-1982	24-Jan-1991
10-Jan-1993	27-Feb-1988	25-Feb-1989	27-Dec-1992	22-Jan-1996	27-Jan-1987	13-Jan-1995	03-Feb-1993	02-Jan-1982	16-Feb-1992
25-Jan-1994	28-Feb-1988	26-Feb-1989	28-Dec-1992	27-Jan-1996	28-Jan-1987	13-Jan-1996	04-Feb-1993	15-Dec-1982	25-Feb-1992
04-Dec-1994	12-Feb-1989	06-Jan-1994	03-Feb-1996	28-Jan-1996	02-Dec-1987	25-Jan-1996	09-Jan-1996	17-Jan-1984	23-Dec-1992
05-Dec-1994	13-Feb-1989	03-Feb-1994	27-Dec-1996	11-Dec-1996	03-Dec-1987	09-Dec-1996	26-Feb-1996	13-Dec-1985	22-Jan-1993
06-Dec-1994	15-Feb-1993	04-Feb-1994	16-Dec-1997	09-Jan-1998	06-Dec-1987	10-Dec-1996	03-Dec-1996	14-Dec-1985	22-Feb-1993
07-Dec-1994	16-Feb-1993	25-Jan-1996	19-Dec-2000	10-Jan-1998	06-Jan-1989	16-Dec-1996	22-Jan-1997	15-Dec-1985	11-Dec-1993
17-Feb-1997	08-Jan-1995	06-Feb-1996	20-Dec-2000	11-Jan-1998	05-Dec-1989	31-Dec-2000	09-Feb-1998	10-Feb-1988	17-Jan-1994
18-Feb-1997	04-Feb-1999	07-Feb-1996	21-Dec-2000	04-Jan-1999	28-Feb-1991	14-Dec-2002	10-Feb-1998	23-Jan-1994	16-Feb-1994
19-Feb-1997	16-Jan-2000	10-Jan-1999	12-Feb-2003	05-Jan-1999	15-Feb-1994	27-Jan-2003	02-Jan-2002	27-Jan-1994	18-Feb-1995
20-Feb-1997	20-Feb-2001	30-Jan-2003	15-Feb-2003	07-Jan-1999	31-Dec-1994	17-Feb-2003	04-Feb-2005	16-Feb-1996	20-Jan-1997
06-Feb-2000	02-Feb-2005	31-Jan-2003	25-Feb-2003	06-Feb-2001	07-Feb-1995	18-Feb-2003	05-Feb-2005	15-Feb-1999	21-Jan-1997
07-Feb-2000	12-Dec-2005	25-Dec-2004	08-Jan-2006	19-Feb-2004	10-Dec-1996	04-Feb-2005	06-Feb-2005	19-Jan-2004	20-Jan-1998
08-Feb-2000	13-Dec-2005	26-Dec-2004	23-Jan-2006	16-Jan-2005	24-Dec-2000	14-Jan-2006	07-Feb-2005	25-Feb-2005	30-Dec-2000
31-Dec-2006	14-Dec-2005	08-Dec-2006	12-Feb-2006	17-Jan-2005	10-Jan-2001	23-Feb-2006	08-Feb-2005	06-Feb-2006	10-Dec-2006

Table V-1: Dates corresponding to the 1% highest scores of PC time series used to build the positive composites of Figures V-2 and V-3.

PC1	PC2	PC3	PC4	PC5	PC6	PC7	PC8	PC9	PC10
05-Feb-1976	05-Jan-1974	16-Dec-1972	12-Jan-1977	07-Jan-1973	18-Jan-1972	18-Dec-1972	07-Feb-1974	17-Jan-1973	24-Jan-1972
26-Dec-1976	23-Feb-1978	27-Feb-1977	13-Jan-1977	08-Jan-1973	23-Jan-1972	05-Jan-1976	23-Feb-1974	20-Dec-1973	26-Jan-1972
09-Feb-1978	24-Feb-1978	28-Feb-1977	14-Jan-1977	19-Feb-1974	28-Dec-1973	04-Feb-1976	25-Feb-1974	21-Dec-1977	24-Feb-1974
10-Feb-1978	25-Feb-1978	19-Dec-1977	13-Feb-1978	02-Jan-1977	08-Feb-1974	09-Dec-1976	02-Dec-1976	20-Jan-1978	20-Jan-1975
11-Feb-1978	26-Feb-1978	20-Dec-1977	14-Feb-1978	03-Feb-1979	27-Jan-1976	10-Dec-1976	10-Dec-1976	04-Jan-1979	23-Dec-1975
12-Feb-1978	27-Feb-1978	21-Dec-1977	29-Jan-1979	15-Feb-1979	06-Feb-1976	14-Dec-1976	11-Dec-1976	27-Dec-1980	24-Dec-1975
13-Feb-1978	07-Dec-1978	14-Feb-1978	04-Dec-1981	16-Feb-1979	07-Feb-1976	29-Dec-1977	17-Feb-1978	24-Feb-1981	23-Feb-1976
14-Feb-1978	11-Dec-1978	15-Feb-1978	05-Dec-1981	23-Jan-1982	27-Feb-1979	30-Dec-1977	16-Jan-1979	15-Dec-1984	28-Feb-1976
17-Jan-1979	12-Dec-1978	16-Feb-1978	04-Jan-1982	26-Feb-1982	18-Jan-1980	16-Jan-1979	03-Dec-1980	16-Dec-1984	11-Dec-1977
18-Jan-1979	13-Dec-1978	26-Jan-1981	05-Jan-1982	09-Feb-1984	28-Jan-1984	25-Jan-1980	15-Jan-1981	17-Dec-1984	16-Jan-1979
19-Jan-1979	11-Feb-1979	21-Jan-1983	15-Jan-1983	13-Jan-1985	09-Feb-1988	26-Jan-1980	30-Jan-1982	08-Feb-1986	27-Dec-1979
21-Jan-1979	12-Feb-1979	22-Jan-1983	01-Feb-1983	14-Jan-1985	20-Jan-1990	10-Dec-1980	31-Jan-1982	28-Feb-1987	21-Jan-1980
22-Jan-1979	13-Feb-1979	23-Jan-1983	19-Dec-1986	14-Jan-1987	21-Jan-1990	19-Jan-1981	23-Dec-1983	15-Jan-1988	05-Dec-1982
23-Jan-1979	18-Dec-1983	23-Feb-1983	14-Feb-1990	15-Jan-1987	21-Dec-1990	07-Feb-1982	02-Jan-1985	03-Jan-1990	01-Feb-1984
24-Jan-1979	19-Dec-1983	05-Feb-1985	22-Dec-1991	05-Jan-1989	22-Dec-1990	25-Dec-1983	03-Jan-1987	24-Dec-1990	16-Jan-1985
25-Jan-1979	20-Dec-1983	01-Dec-1985	23-Dec-1991	11-Dec-1990	23-Dec-1990	26-Dec-1983	11-Jan-1987	01-Feb-1991	28-Feb-1985
26-Jan-1979	21-Dec-1983	22-Jan-1987	30-Dec-1994	12-Dec-1990	12-Jan-1994	22-Jan-1985	23-Feb-1988	16-Dec-1991	15-Dec-1985
27-Jan-1979	25-Feb-1989	23-Jan-1987	13-Dec-1996	08-Dec-1992	17-Jan-1994	23-Jan-1985	24-Feb-1988	31-Jan-1992	16-Dec-1985
07-Jan-1985	26-Feb-1989	24-Jan-1987	27-Feb-1998	03-Dec-1995	18-Jan-1994	04-Dec-1985	25-Feb-1988	20-Dec-1992	04-Jan-1987
21-Jan-1996	13-Dec-1989	25-Feb-1987	28-Feb-1998	27-Feb-1996	05-Feb-1998	28-Dec-1989	16-Feb-1990	21-Dec-1992	09-Feb-1988
22-Jan-1996	14-Dec-1989	27-Dec-1987	10-Dec-1999	28-Feb-1996	15-Jan-1999	05-Dec-1991	13-Dec-1990	22-Dec-1992	02-Jan-1990
27-Jan-1996	15-Dec-1989	29-Dec-1988	11-Dec-1999	15-Dec-1999	27-Dec-2001	03-Feb-1992	04-Dec-1991	22-Jan-1996	18-Jan-1991
28-Jan-1996	16-Dec-1989	30-Dec-1988	12-Dec-1999	16-Dec-1999	22-Feb-2002	23-Dec-1998	25-Dec-1993	23-Jan-1996	01-Feb-1991
29-Jan-1996	17-Dec-1989	04-Feb-1990	13-Dec-1999	06-Feb-2002	25-Feb-2002	12-Jan-1999	20-Feb-1994	28-Jan-1996	14-Feb-1993
30-Jan-1996	30-Dec-1995	13-Jan-1992	14-Dec-1999	09-Jan-2003	22-Dec-2004	30-Dec-1999	20-Feb-1996	20-Jan-1997	14-Jan-1996
01-Feb-1998	31-Dec-1995	14-Jan-1992	26-Feb-2001	10-Jan-2003	23-Dec-2004	08-Jan-2002	25-Dec-1996	03-Feb-1998	28-Feb-1996
02-Feb-1998	05-Jan-1996	10-Feb-1998	27-Feb-2001	23-Jan-2003	24-Dec-2004	20-Feb-2004	20-Dec-1998	04-Feb-1998	18-Jan-1997
03-Feb-1998	06-Jan-1996	11-Feb-1998	28-Feb-2001	25-Jan-2003	17-Jan-2005	18-Jan-2005	24-Jan-2002	20-Dec-1998	13-Jan-2000
27-Feb-2001	07-Jan-1996	12-Feb-1998	24-Dec-2001	18-Jan-2004	19-Jan-2005	08-Feb-2006	21-Dec-2003	26-Jan-1999	11-Feb-2001
28-Feb-2001	08-Jan-1996	13-Feb-1998	25-Dec-2001	25-Jan-2005	04-Jan-2006	11-Jan-2007	22-Dec-2003	26-Feb-2000	16-Dec-2002
19-Feb-2004	09-Jan-1996	11-Jan-2002	26-Dec-2001	26-Jan-2005	13-Dec-2006	27-Jan-2007	23-Dec-2003	27-Feb-2000	22-Jan-2006
20-Feb-2004	23-Jan-2001	02-Feb-2004	23-Feb-2002	20-Feb-2007	21-Feb-2007	28-Jan-2007	17-Dec-2005	18-Jan-2001	17-Dec-2006

Table V-2: Dates corresponding to the 1% lowest scores of PC time series used to build the negative composites of Figures V-2 and V-3.

PC1	PC2	PC3	PC4	PC5	PC6	PC7	PC8	PC9	PC10
21-Jan-1971	18-Jan-1972	06-Feb-1971	26-Jan-1971	17-Jan-1972	28-Jan-1972	23-Jan-1971	21-Jan-1971	09-Dec-1970	08-Dec-1970
16-Feb-1971	21-Jan-1972	17-Jan-1972	23-Feb-1972	26-Jan-1972	04-Feb-1972	11-Feb-1972	13-Jan-1972	20-Jan-1971	04-Dec-1971
17-Feb-1971	22-Jan-1973	22-Feb-1972	11-Dec-1973	31-Jan-1973	05-Feb-1972	17-Jan-1973	03-Feb-1972	21-Jan-1971	17-Jan-1972
11-Feb-1972	31-Jan-1973	17-Jan-1973	24-Dec-1973	14-Feb-1973	06-Feb-1972	21-Jan-1973	22-Jan-1973	06-Feb-1971	09-Feb-1972
25-Feb-1973	30-Dec-1973	26-Feb-1976	28-Dec-1973	25-Feb-1973	20-Feb-1973	11-Feb-1973	11-Feb-1973	16-Feb-1971	17-Jan-1973
06-Feb-1974	04-Feb-1974	14-Dec-1977	06-Jan-1974	14-Jan-1974	19-Dec-1973	15-Feb-1973	03-Feb-1974	05-Dec-1971	02-Feb-1973
18-Jan-1975	13-Dec-1974	07-Jan-1979	07-Jan-1974	06-Feb-1974	14-Jan-1975	19-Feb-1973	23-Feb-1974	03-Feb-1972	13-Feb-1973
01-Dec-1976	19-Jan-1975	27-Jan-1979	29-Dec-1977	17-Feb-1974	15-Jan-1975	21-Dec-1973	06-Dec-1974	11-Feb-1972	14-Feb-1973
02-Dec-1976	20-Jan-1978	09-Dec-1980	07-Jan-1979	15-Feb-1975	22-Feb-1975	24-Feb-1974	20-Jan-1978	12-Feb-1972	28-Feb-1973
03-Dec-1976	27-Dec-1980	31-Jan-1981	13-Feb-1979	09-Dec-1980	28-Feb-1975	15-Jan-1975	06-Feb-1978	17-Jan-1973	03-Dec-1973
20-Jan-1978	20-Jan-1981	14-Feb-1981	27-Feb-1980	20-Dec-1980	23-Feb-1978	02-Dec-1976	05-Dec-1978	05-Jan-1974	20-Dec-1973
28-Jan-1978	19-Dec-1981	22-Dec-1981	14-Jan-1982	25-Feb-1982	13-Jan-1979	12-Jan-1977	11-Jan-1979	14-Jan-1975	29-Dec-1973
13-Dec-1978	18-Dec-1982	21-Jan-1983	17-Jan-1988	27-Feb-1982	19-Jan-1979	14-Jan-1977	05-Feb-1979	24-Jan-1978	21-Feb-1974
31-Dec-1978	08-Feb-1984	22-Jan-1985	06-Feb-1988	21-Jan-1983	13-Feb-1979	29-Dec-1977	15-Feb-1979	26-Feb-1978	22-Feb-1974
11-Jan-1979	09-Jan-1986	23-Feb-1985	16-Feb-1988	07-Jan-1984	20-Jan-1981	28-Feb-1978	13-Jan-1981	28-Feb-1978	25-Feb-1974
28-Dec-1980	15-Jan-1986	14-Feb-1986	11-Feb-1989	14-Jan-1984	05-Feb-1981	15-Dec-1978	16-Jan-1981	09-Jan-1979	15-Dec-1978
12-Dec-1981	31-Jan-1986	10-Jan-1987	25-Feb-1989	23-Feb-1984	15-Feb-1988	05-Feb-1979	20-Jan-1981	05-Feb-1979	28-Dec-1980
13-Dec-1981	26-Dec-1986	11-Feb-1987	01-Feb-1990	23-Jan-1986	16-Feb-1988	09-Feb-1979	19-Dec-1981	09-Feb-1979	17-Feb-1981
18-Dec-1981	11-Jan-1987	09-Dec-1987	21-Jan-1991	12-Feb-1987	26-Feb-1989	24-Feb-1979	22-Dec-1983	15-Feb-1979	07-Jan-1986
12-Feb-1985	16-Jan-1987	11-Feb-1989	19-Feb-1992	23-Jan-1988	19-Dec-1992	31-Dec-1979	09-Feb-1984	23-Feb-1982	16-Dec-1986
29-Jan-1988	11-Dec-1990	12-Feb-1989	20-Feb-1992	09-Feb-1988	06-Jan-1995	16-Dec-1980	11-Jan-1987	20-Jan-1983	10-Jan-1987
30-Jan-1988	13-Dec-1990	03-Dec-1989	31-Jan-1993	13-Feb-1990	30-Dec-1995	09-Jan-1984	25-Feb-1989	18-Feb-1983	22-Jan-1988
25-Feb-1989	08-Dec-1992	20-Dec-1990	01-Feb-1993	15-Jan-1994	15-Jan-1996	01-Dec-1984	14-Dec-1989	02-Feb-1991	13-Feb-1993
26-Feb-1989	09-Dec-1992	30-Dec-1995	24-Jan-1995	05-Feb-1994	21-Dec-1996	31-Dec-1984	15-Dec-1989	08-Dec-1991	26-Dec-1994
12-Feb-1990	12-Jan-1995	23-Jan-1996	10-Jan-1997	14-Feb-1997	16-Jan-1997	27-Jan-1990	10-Dec-1990	10-Dec-1991	12-Jan-1995
07-Feb-1996	08-Feb-1996	12-Dec-1996	15-Jan-1997	20-Jan-1998	10-Jan-1998	17-Jan-1994	27-Feb-1993	11-Dec-1991	18-Jan-1995
27-Dec-1999	21-Dec-1998	20-Dec-1996	25-Jan-1997	07-Feb-2000	30-Dec-1998	26-Feb-1994	02-Jan-1995	13-Feb-1992	13-Feb-1995
28-Jan-2001	10-Feb-1999	05-Dec-1997	26-Feb-1999	28-Jan-2001	22-Dec-2000	30-Dec-1998	26-Dec-1996	27-Feb-1996	30-Jan-1999

Table V-3: Dates corresponding to the 1% highest scores of PC time series used to build the positive composites of Figures V-4 and V-5.

PC1	PC2	PC3	PC4	PC5	PC6	PC7	PC8	PC9	PC10
02-Dec-1970	26-Jan-1971	26-Jan-1971	26-Feb-1973	09-Dec-1970	03-Dec-1976	14-Feb-1972	06-Feb-1972	15-Dec-1970	05-Dec-1975
13-Feb-1971	05-Feb-1972	24-Feb-1973	02-Dec-1976	05-Dec-1971	20-Dec-1976	24-Feb-1972	24-Feb-1972	22-Jan-1973	04-Jan-1977
14-Feb-1971	26-Dec-1972	25-Jan-1977	31-Dec-1976	12-Feb-1972	21-Dec-1976	09-Feb-1975	02-Feb-1975	09-Dec-1973	05-Jan-1977
20-Dec-1971	05-Jan-1974	27-Jan-1978	21-Dec-1977	14-Feb-1972	12-Jan-1977	16-Dec-1975	27-Feb-1976	03-Feb-1974	14-Jan-1977
23-Dec-1971	14-Jan-1975	28-Dec-1978	23-Feb-1978	07-Feb-1974	14-Jan-1977	05-Feb-1976	02-Dec-1976	27-Jan-1976	07-Dec-1977
25-Dec-1971	06-Dec-1976	30-Jan-1979	18-Jan-1979	02-Dec-1976	10-Jan-1979	07-Feb-1976	20-Dec-1976	30-Jan-1976	13-Dec-1977
27-Dec-1971	07-Dec-1976	13-Dec-1979	19-Jan-1979	07-Jan-1977	05-Feb-1979	11-Dec-1978	21-Dec-1976	01-Dec-1976	15-Dec-1977
28-Feb-1972	31-Dec-1976	27-Dec-1979	31-Jan-1981	06-Jan-1979	14-Jan-1980	27-Dec-1979	06-Jan-1977	26-Jan-1979	17-Dec-1977
26-Jan-1973	23-Feb-1978	12-Dec-1981	27-Feb-1981	27-Jan-1979	11-Dec-1981	11-Jan-1981	07-Jan-1977	05-Feb-1981	19-Jan-1978
16-Dec-1973	28-Feb-1978	06-Jan-1982	29-Dec-1981	14-Feb-1979	16-Dec-1981	28-Dec-1981	17-Feb-1977	10-Dec-1981	25-Feb-1978
21-Jan-1974	08-Dec-1978	07-Feb-1983	15-Feb-1982	14-Jan-1980	23-Dec-1981	15-Jan-1982	23-Feb-1977	13-Dec-1981	06-Feb-1979
22-Jan-1974	10-Dec-1978	23-Dec-1983	21-Jan-1983	20-Feb-1980	24-Dec-1981	27-Jan-1982	06-Dec-1977	14-Dec-1981	15-Feb-1979
28-Feb-1974	11-Dec-1978	07-Feb-1984	07-Feb-1983	21-Feb-1980	17-Jan-1982	01-Dec-1983	16-Dec-1978	21-Dec-1981	16-Feb-1979
24-Feb-1975	27-Dec-1978	31-Dec-1986	09-Feb-1984	28-Dec-1980	28-Jan-1982	17-Jan-1985	19-Jan-1979	23-Dec-1981	17-Feb-1979
11-Dec-1976	28-Dec-1978	15-Jan-1987	10-Jan-1987	30-Dec-1980	11-Dec-1982	21-Jan-1985	14-Dec-1979	30-Dec-1981	19-Feb-1980
12-Dec-1976	30-Dec-1978	11-Feb-1988	14-Jan-1987	14-Jan-1982	12-Dec-1982	26-Jan-1985	21-Feb-1980	15-Jan-1984	27-Dec-1980
13-Dec-1976	30-Dec-1981	24-Feb-1988	15-Jan-1987	09-Feb-1984	16-Jan-1986	28-Feb-1986	20-Dec-1982	09-Feb-1985	18-Jan-1981
19-Dec-1976	21-Jan-1985	03-Dec-1988	11-Feb-1987	03-Dec-1987	23-Jan-1986	10-Jan-1987	12-Jan-1984	12-Feb-1985	12-Feb-1981
22-Dec-1976	14-Dec-1989	06-Feb-1990	03-Dec-1987	25-Feb-1988	19-Dec-1986	21-Jan-1987	14-Jan-1984	13-Dec-1987	26-Feb-1982
27-Dec-1976	15-Dec-1989	11-Feb-1990	04-Dec-1987	13-Dec-1988	13-Jan-1987	11-Feb-1987	12-Feb-1990	26-Jan-1990	16-Dec-1983
28-Dec-1976	16-Dec-1989	12-Feb-1990	09-Dec-1987	23-Jan-1991	18-Jan-1988	04-Dec-1987	03-Feb-1991	09-Jan-1994	30-Dec-1984
29-Dec-1976	20-Dec-1989	13-Feb-1990	13-Dec-1987	03-Feb-1991	19-Feb-1991	09-Dec-1987	03-Jan-1994	10-Jan-1994	23-Jan-1985
26-Dec-1977	21-Dec-1989	10-Dec-1990	27-Feb-1988	19-Feb-1991	05-Dec-1992	27-Jan-1988	05-Jan-1994	03-Feb-1994	25-Dec-1985
13-Feb-1980	01-Dec-2000	10-Jan-1991	20-Dec-1991	28-Jan-1992	06-Dec-1992	14-Dec-1989	21-Jan-1996	18-Jan-1995	21-Feb-1986
14-Feb-1980	07-Dec-2000	20-Dec-1991	21-Jan-1996	20-Feb-1992	06-Jan-1994	15-Dec-1989	01-Feb-1996	20-Jan-1995	09-Jan-1990
02-Dec-1982	01-Jan-2001	11-Jan-1993	22-Jan-1996	20-Jan-1994	01-Jan-1995	16-Dec-1989	14-Jan-1997	06-Feb-1996	11-Dec-1990
14-Feb-1983	06-Feb-2001	19-Jan-1995	01-Feb-1996	01-Feb-1996	12-Dec-1999	22-Feb-1999	12-Dec-1999	20-Dec-1996	08-Dec-1992
27-Feb-1992	07-Feb-2001	27-Dec-1999	17-Dec-1997	15-Feb-2001	26-Dec-1999	31-Dec-2000	22-Dec-2000	04-Feb-1998	06-Jan-1995

Table V-4: Dates corresponding to the 1% lowest scores of PC time series used to build the negative composites of Figures V-4 and V-5.

PC1	PC2	PC3	PC4	PC5	PC6	PC7	PC8	PC9	PC10
26-Feb-1962	15-Jan-1972	09-Feb-1960	16-Feb-1959	18-Feb-1961	08-Dec-1959	21-Feb-1959	02-Dec-1958	22-Jan-1964	16-Feb-1959
27-Feb-1962	17-Jan-1972	24-Dec-1962	17-Feb-1959	19-Feb-1961	26-Jan-1960	23-Jan-1961	19-Jan-1959	19-Dec-1964	07-Feb-1962
28-Feb-1962	18-Jan-1972	22-Dec-1964	15-Feb-1961	17-Feb-1962	27-Jan-1960	02-Jan-1962	20-Jan-1959	20-Dec-1964	01-Jan-1963
02-Feb-1963	28-Jan-1972	23-Dec-1964	16-Feb-1961	20-Feb-1962	28-Jan-1960	03-Jan-1962	21-Jan-1959	17-Dec-1965	30-Jan-1967
03-Feb-1963	29-Jan-1972	24-Dec-1964	17-Feb-1961	20-Jan-1967	10-Feb-1962	18-Jan-1963	22-Jan-1959	18-Dec-1965	16-Jan-1968
04-Feb-1963	30-Jan-1972	25-Dec-1964	11-Jan-1964	21-Jan-1967	04-Feb-1968	19-Jan-1963	31-Dec-1961	13-Dec-1966	08-Feb-1969
27-Jan-1966	18-Dec-1972	10-Feb-1965	12-Jan-1964	04-Jan-1968	05-Feb-1968	06-Dec-1963	28-Dec-1962	14-Dec-1966	30-Dec-1969
28-Jan-1966	19-Dec-1972	21-Jan-1968	13-Jan-1964	15-Feb-1970	06-Feb-1968	01-Feb-1965	17-Jan-1963	15-Dec-1966	22-Feb-1973
04-Jan-1969	20-Dec-1972	28-Feb-1970	14-Jan-1964	16-Feb-1970	09-Feb-1969	29-Dec-1970	23-Jan-1963	24-Dec-1967	23-Jan-1976
05-Jan-1969	15-Dec-1976	04-Feb-1971	15-Jan-1964	26-Dec-1977	10-Feb-1969	22-Feb-1972	24-Jan-1963	02-Feb-1969	10-Feb-1976
19-Jan-1969	03-Jan-1977	05-Feb-1971	21-Jan-1964	02-Jan-1981	11-Feb-1969	20-Dec-1973	08-Feb-1965	03-Feb-1969	01-Jan-1977
12-Feb-1969	04-Jan-1977	03-Jan-1975	22-Jan-1964	04-Jan-1981	14-Feb-1969	23-Dec-1973	15-Jan-1968	20-Dec-1971	02-Jan-1977
13-Jan-1977	16-Jan-1979	04-Jan-1975	01-Jan-1972	10-Feb-1981	31-Jan-1971	24-Dec-1973	19-Jan-1969	25-Dec-1977	06-Jan-1977
14-Jan-1977	17-Jan-1979	08-Dec-1975	15-Dec-1972	11-Feb-1981	31-Dec-1972	17-Dec-1975	28-Jan-1969	05-Jan-1979	20-Jan-1977
15-Jan-1977	15-Dec-1984	12-Dec-1975	16-Dec-1972	21-Jan-1982	01-Jan-1973	25-Jan-1976	29-Jan-1969	30-Jan-1979	06-Feb-1977
16-Jan-1977	16-Dec-1984	13-Dec-1975	20-Dec-1977	31-Jan-1982	17-Dec-1976	23-Feb-1977	18-Feb-1969	31-Jan-1979	22-Feb-1977
08-Feb-1978	29-Dec-1984	14-Dec-1975	21-Dec-1977	29-Dec-1982	05-Jan-1977	12-Jan-1978	06-Feb-1970	01-Feb-1979	11-Jan-1978
09-Feb-1978	31-Jan-1986	15-Dec-1975	22-Dec-1977	28-Jan-1983	10-Jan-1977	13-Jan-1978	12-Feb-1971	21-Feb-1983	24-Jan-1980
10-Feb-1978	01-Feb-1986	21-Dec-1975	06-Feb-1985	01-Jan-1985	11-Jan-1977	13-Feb-1981	13-Feb-1971	22-Feb-1983	11-Jan-1981
11-Feb-1978	02-Feb-1986	22-Dec-1975	01-Dec-1985	16-Feb-1985	12-Jan-1977	11-Jan-1982	04-Feb-1976	23-Feb-1983	01-Jan-1983
12-Feb-1978	28-Dec-1989	27-Dec-1975	02-Dec-1985	17-Feb-1985	04-Feb-1978	12-Jan-1982	11-Feb-1981	27-Feb-1983	06-Feb-1983
13-Feb-1978	02-Feb-1991	31-Dec-1975	04-Dec-1986	16-Dec-1985	28-Jan-1984	12-Feb-1983	13-Feb-1981	28-Feb-1983	27-Feb-1983
20-Jan-1979	03-Feb-1991	06-Jan-1977	05-Dec-1986	17-Dec-1985	14-Feb-1984	27-Dec-1985	14-Feb-1981	15-Dec-1984	26-Jan-1984
21-Jan-1979	04-Feb-1991	26-Feb-1979	27-Dec-1987	18-Dec-1985	18-Feb-1984	28-Dec-1985	29-Dec-1981	16-Dec-1984	13-Dec-1984
23-Jan-1979	05-Feb-1991	11-Jan-1981	28-Dec-1987	15-Jan-1986	20-Feb-1984	29-Dec-1985	03-Feb-1982	17-Dec-1984	31-Jan-1986
24-Jan-1979	06-Feb-1991	03-Dec-1981	30-Dec-1988	16-Jan-1986	21-Feb-1984	27-Jan-1987	04-Feb-1982	18-Dec-1984	20-Dec-1986
29-Dec-1981	06-Dec-1991	27-Feb-1988	03-Jan-1989	20-Dec-1986	25-Dec-1985	28-Jan-1987	05-Feb-1982	19-Dec-1984	12-Jan-1987
30-Dec-1981	07-Dec-1991	08-Dec-1988	04-Jan-1989	31-Dec-1988	27-Jan-1986	29-Jan-1987	06-Feb-1982	22-Dec-1986	13-Jan-1987
31-Dec-1981	12-Feb-1994	02-Dec-1990	30-Jan-1989	30-Dec-1991	28-Jan-1986	01-Dec-1988	01-Feb-1988	23-Dec-1986	06-Dec-1987
17-Jan-1985	13-Feb-1994	06-Dec-1990	03-Dec-1989	16-Feb-1992	05-Feb-1988	24-Feb-1989	17-Jan-1996	07-Jan-1987	17-Jan-1988
18-Jan-1985	04-Dec-1995	28-Jan-1992	04-Dec-1989	17-Feb-1992	15-Feb-1989	07-Dec-1989	21-Jan-1996	08-Jan-1987	31-Dec-1991
19-Jan-1985	05-Dec-1995	27-Jan-1997	04-Jan-1992	27-Dec-1992	25-Jan-1990	17-Feb-1991	22-Jan-1996	24-Feb-1988	24-Feb-1992
20-Jan-1985	15-Jan-1996	28-Jan-1997	05-Jan-1992	09-Feb-1993	18-Jan-1995	18-Feb-1991	27-Jan-1996	18-Jan-1989	03-Feb-1993
10-Dec-1996	16-Jan-1996	15-Feb-1999	05-Feb-1993	28-Jan-1994	19-Jan-1995	05-Feb-1993	25-Jan-1997	09-Jan-1992	27-Feb-1994
11-Dec-1996	15-Dec-1997	01-Dec-1999	09-Feb-1993	29-Jan-1994	20-Jan-1995	06-Feb-1993	09-Jan-1998	12-Jan-1992	10-Feb-1996
25-Feb-2001	16-Dec-1997	16-Jan-2000	17-Dec-1995	11-Jan-1995	21-Jan-1995	17-Jan-1994	10-Jan-1998	13-Jan-1992	12-Jan-1998
26-Feb-2001	07-Dec-2001	17-Jan-2000	17-Dec-1997	12-Jan-1995	22-Jan-1995	09-Feb-1995	11-Jan-1998	11-Dec-1997	07-Jan-2002
27-Feb-2001	08-Dec-2001	08-Jan-2002	11-Feb-1998	31-Jan-1997	24-Jan-1996	10-Feb-1995	07-Jan-1999	12-Dec-1997	08-Jan-2002
23-Feb-2005	05-Dec-2002	19-Feb-2004	12-Feb-1998	31-Jan-2001	25-Jan-1996	03-Feb-1996	07-Jan-2002	04-Feb-1998	03-Feb-2003
24-Feb-2005	06-Dec-2002	20-Feb-2004	13-Feb-1998	01-Feb-2001	09-Dec-1996	21-Dec-1996	11-Feb-2002	12-Feb-1998	04-Feb-2005
25-Feb-2005	07-Dec-2002	12-Dec-2005	14-Feb-1998	28-Jan-2003	10-Dec-1996	22-Dec-1996	18-Feb-2004	22-Dec-2001	05-Feb-2005
26-Feb-2005	04-Jan-2006	14-Dec-2005	11-Jan-2002	29-Jan-2003	15-Jan-1998	20-Jan-1997	19-Feb-2004	15-Feb-2005	12-Feb-2005
27-Feb-2005	08-Jan-2006	15-Dec-2005	12-Jan-2002	30-Jan-2003	06-Feb-2001	21-Jan-1997	16-Jan-2005	23-Jan-2007	16-Jan-2006
27-Feb-2006	22-Jan-2006	25-Jan-2007	28-Dec-2006	24-Dec-2006	30-Dec-2005	30-Jan-2003	17-Jan-2005	24-Jan-2007	25-Feb-2007

Table V-5: Dates corresponding to the 1% highest scores of PC time series used to build the positive composites of Figures V-6 and V-7.

PC1	PC2	PC3	PC4	PC5	PC6	PC7	PC8	PC9	PC10
14-Feb-1959	01-Dec-1961	14-Dec-1958	04-Dec-1959	13-Feb-1960	26-Jan-1961	10-Feb-1961	12-Jan-1960	25-Dec-1962	01-Dec-1962
15-Feb-1959	02-Dec-1961	01-Dec-1959	24-Dec-1960	24-Feb-1964	14-Dec-1961	30-Dec-1964	13-Jan-1960	22-Jan-1963	02-Dec-1962
26-Feb-1959	13-Feb-1962	20-Feb-1966	25-Dec-1960	25-Feb-1964	21-Dec-1961	31-Dec-1964	14-Jan-1960	23-Jan-1963	03-Dec-1962
27-Feb-1959	16-Feb-1962	21-Feb-1966	13-Dec-1962	28-Jan-1965	22-Dec-1961	27-Jan-1966	15-Jan-1960	10-Feb-1963	01-Jan-1964
28-Feb-1959	06-Dec-1967	22-Feb-1966	16-Dec-1962	29-Jan-1965	28-Jan-1962	28-Jan-1966	14-Feb-1962	01-Dec-1963	21-Jan-1964
16-Jan-1965	07-Dec-1967	23-Jan-1971	17-Dec-1962	20-Feb-1969	18-Dec-1962	29-Jan-1966	04-Jan-1965	30-Dec-1963	31-Jan-1964
17-Jan-1965	04-Feb-1970	01-Feb-1972	18-Dec-1962	21-Feb-1969	19-Dec-1962	10-Dec-1966	19-Feb-1965	19-Jan-1965	26-Dec-1964
28-Feb-1967	13-Feb-1973	02-Feb-1972	19-Jan-1965	01-Jan-1970	22-Dec-1962	16-Dec-1966	20-Feb-1965	16-Jan-1967	11-Feb-1965
09-Feb-1976	22-Feb-1973	03-Feb-1972	20-Jan-1965	02-Jan-1970	10-Feb-1967	17-Dec-1966	21-Dec-1965	17-Jan-1967	30-Dec-1965
10-Feb-1976	23-Feb-1973	05-Jan-1974	21-Jan-1965	08-Jan-1971	13-Jan-1968	22-Dec-1968	16-Dec-1967	13-Feb-1967	31-Dec-1965
24-Feb-1976	06-Jan-1975	06-Jan-1974	20-Jan-1972	10-Jan-1971	19-Feb-1968	23-Dec-1968	26-Feb-1968	04-Jan-1969	24-Feb-1966
25-Feb-1976	21-Jan-1976	09-Jan-1974	21-Jan-1972	17-Jan-1971	09-Jan-1973	24-Dec-1968	01-Dec-1969	05-Jan-1969	13-Jan-1967
01-Jan-1983	22-Jan-1976	28-Jan-1974	13-Feb-1973	21-Jan-1971	10-Jan-1973	17-Jan-1969	02-Dec-1969	14-Feb-1973	05-Jan-1971
02-Jan-1983	23-Jan-1976	07-Dec-1977	14-Feb-1973	15-Jan-1975	11-Jan-1973	18-Jan-1969	28-Dec-1972	22-Feb-1974	06-Jan-1971
03-Jan-1983	02-Dec-1976	08-Dec-1977	15-Feb-1973	05-Feb-1976	12-Jan-1973	19-Jan-1969	07-Jan-1973	06-Feb-1975	08-Jan-1971
04-Jan-1983	03-Jan-1981	10-Dec-1978	16-Feb-1973	06-Feb-1976	13-Jan-1973	20-Jan-1969	08-Jan-1973	29-Dec-1976	09-Jan-1971
05-Jan-1983	08-Dec-1981	11-Dec-1978	26-Jan-1976	23-Feb-1978	04-Feb-1976	21-Jan-1969	13-Dec-1973	03-Feb-1982	03-Feb-1973
06-Jan-1983	09-Dec-1981	12-Dec-1978	27-Jan-1976	24-Feb-1978	03-Dec-1977	22-Jan-1969	19-Feb-1974	15-Dec-1983	23-Feb-1974
07-Jan-1983	10-Dec-1981	13-Dec-1978	02-Dec-1976	25-Feb-1978	04-Dec-1977	26-Jan-1969	02-Jan-1977	13-Jan-1984	18-Feb-1975
25-Jan-1983	16-Dec-1982	19-Dec-1983	03-Dec-1976	26-Feb-1978	06-Feb-1979	27-Jan-1969	15-Feb-1979	28-Feb-1986	26-Dec-1975
26-Jan-1983	17-Dec-1982	20-Dec-1983	15-Jan-1981	04-Feb-1979	07-Feb-1979	16-Feb-1969	16-Feb-1979	01-Feb-1988	27-Jan-1976
27-Dec-1983	15-Jan-1983	13-Dec-1986	16-Jan-1981	21-Dec-1979	08-Feb-1979	17-Feb-1969	19-Jan-1981	16-Dec-1988	14-Feb-1978
14-Jan-1989	18-Jan-1983	14-Dec-1986	05-Feb-1981	30-Jan-1987	09-Feb-1979	04-Dec-1974	21-Jan-1982	31-Dec-1989	24-Feb-1979
27-Jan-1989	29-Jan-1983	15-Dec-1986	24-Jan-1984	14-Dec-1987	10-Feb-1979	05-Feb-1978	22-Jan-1982	05-Jan-1993	20-Jan-1982
28-Jan-1989	30-Jan-1983	28-Jan-1988	05-Feb-1984	15-Dec-1987	11-Feb-1979	25-Dec-1979	13-Jan-1985	06-Jan-1993	23-Jan-1982
04-Feb-1989	01-Feb-1983	29-Jan-1988	30-Jan-1986	14-Dec-1989	26-Jan-1981	26-Dec-1979	14-Jan-1985	07-Feb-1995	24-Jan-1982
11-Feb-1989	03-Jan-1984	25-Feb-1989	31-Jan-1986	15-Dec-1989	23-Jan-1983	09-Feb-1980	16-Jan-1985	31-Jan-1996	10-Jan-1983
12-Feb-1989	26-Feb-1990	24-Dec-1989	09-Feb-1988	16-Dec-1989	11-Jan-1985	23-Feb-1981	14-Jan-1987	01-Feb-1996	14-Dec-1985
20-Feb-1990	27-Feb-1990	31-Jan-1990	25-Feb-1989	17-Dec-1989	18-Dec-1985	24-Feb-1981	15-Jan-1987	27-Dec-1996	31-Jan-1987
24-Feb-1990	28-Feb-1990	14-Feb-1995	26-Feb-1989	28-Dec-1989	25-Dec-1988	25-Feb-1981	14-Feb-1987	26-Jan-1998	03-Jan-1988
25-Feb-1990	12-Jan-1993	06-Jan-1996	27-Feb-1989	04-Feb-1990	05-Dec-1991	04-Jan-1982	05-Jan-1989	02-Dec-1998	20-Jan-1990
26-Feb-1990	23-Jan-1993	07-Jan-1996	22-Feb-1993	05-Feb-1990	17-Jan-1992	20-Dec-1984	06-Jan-1989	22-Dec-2000	28-Dec-1990
26-Dec-1990	24-Jan-1993	01-Jan-1998	05-Feb-1996	06-Feb-1990	18-Jan-1992	26-Dec-1986	11-Dec-1990	08-Dec-2002	28-Jan-1992
27-Dec-1990	30-Dec-1994	02-Jan-1998	06-Feb-1996	07-Feb-1990	19-Jan-1992	05-Jan-1987	12-Dec-1990	09-Dec-2002	28-Dec-1992
28-Dec-1990	31-Dec-1994	03-Jan-1998	07-Feb-1996	20-Feb-1990	30-Jan-1992	17-Dec-1994	28-Feb-1996	19-Feb-2003	28-Jan-1994
17-Dec-1991	25-Jan-1995	22-Jan-2001	08-Feb-1996	30-Dec-1995	18-Jan-2000	09-Feb-1998	09-Jan-2003	24-Feb-2003	11-Jan-1997
18-Dec-1991	07-Feb-1995	23-Jan-2001	31-Jan-2003	31-Dec-1995	13-Feb-2002	10-Feb-1998	10-Jan-2003	04-Dec-2003	05-Feb-1998
09-Jan-1993	08-Feb-1995	24-Jan-2001	01-Feb-2003	01-Jan-1996	19-Feb-2003	26-Feb-1998	11-Jan-2003	15-Dec-2004	01-Feb-2002
10-Jan-1993	09-Feb-1995	23-Dec-2002	22-Jan-2004	06-Jan-1996	21-Jan-2004	19-Feb-1999	23-Jan-2003	11-Jan-2006	10-Feb-2002
22-Jan-1993	27-Feb-1998	24-Dec-2002	19-Dec-2004	07-Jan-1996	22-Jan-2004	04-Dec-2001	24-Jan-2003	13-Feb-2006	17-Feb-2003
06-Feb-2000	28-Feb-1998	27-Dec-2002	23-Dec-2004	08-Jan-1996	23-Jan-2004	05-Dec-2001	25-Jan-2003	14-Feb-2006	12-Dec-2003
07-Feb-2000	05-Feb-1999	20-Feb-2007	27-Jan-2005	09-Jan-1996	28-Jan-2007	03-Feb-2005	30-Dec-2003	22-Dec-2006	24-Dec-2003
30-Dec-2006	23-Feb-2002	21-Feb-2007	28-Jan-2005	10-Jan-1996	29-Jan-2007	09-Feb-2005	25-Jan-2005	26-Dec-2006	25-Dec-2003
31-Dec-2006	19-Jan-2007	22-Feb-2007	15-Feb-2005	20-Feb-2004	30-Jan-2007	24-Feb-2007	24-Feb-2006	27-Dec-2006	31-Jan-2006

Table V-6: Dates corresponding to the 1% lowest scores of PC time series used to build the negative composites of Figures V-6 and V-7.

References

Allison, I., R. G. Barry and B. E. Goodison (2000). *Climate and Cryosphere (CLIC) Project*, Science and coordination Plan, Version I. World Climate Research Programme, International Council for Science, Intergovernmental Oceanographic Commission, World Meteorological Organization. 73 pp.

Barnston, A. G. and R. E. Livezey (1987). Classification, seasonality and persistence of low-frequency atmospheric circulation patterns. *Month. Wea. Rev.*, **115,** 1083-1126.

Bluestein H B. 1993. Synoptic Dynamic Meteorology in Midlatitudes.Vol. II. Observations and Theory of Weather Systems. Oxford University Press. pp594.

Bojariu, R. (1997). Climate variability modes due to ocean-atmosphere interaction in the central Atlantic. *Tellus*, **49A**, 362-370.

Bonan, G. B., D. Pollard and S. L. Thompson (1992). Effects of boreal forest vegetation on global climate. *Nature*, **359**, 716-718.

Brazdil R. and A. N. Zolotokfylin (1995). The QBO signal in monthly precipitation fields over Europe. *Theor. Appl. Climatol.*, **51**, 2-12.

Calov, R., R. Greve and K. Hutter (2003). Climate reconstruction from ice core isotope analysis. *Geophys. Res. Abs.*, **5**, 795.

Hurrel, J. W. (1995). Decadal trends in the North Atlantic Oscillation: regional temperatures and precipitation. *Science*, **269**, 676-679.

Hurrell, J. W. and H. van Loon (1997). Decadal variations in climate associated with the North Atlantic Oscillation. *Climate Change*, **36**, 301–326.

IPCC Technical Summary. Climate Change (2001). *Impacts, Adaptation and Vulnerability. A Report of Working Group II of the Intergovernmental Panel on Climate Change*. J J. McCarthy, O F. Canziani, N A. Leary, D J. Dokken and K S. White (Eds). Cambridge University Press. 1000 pp.

IPCC Climate Change: The Scientific Basis (2001). Contribution of working group I to the thirth assessment report of the Intergovernmental Panel on Climate Change. Cambridge University Press.

IPCC Policy Makers, Summary for Policy Makers (2001). A report of Working Group I of the Intergovernmental Pannel on Climate Change. Albritton et al.Geneva, Switzerland. 98 pp.

Jacobeit, J., H. Wanner, J. Luterbacher, C. Beck, A. Philipp and K. Sturm (2003). Atmospheric circulation variability in the North-Atlantic-European area since the mid-seventeenth century. *Clim. Dyn*. **20**, 341-352.

Jiang, N., J. D. Neelin and M. Ghil (1995). Quasi-quadriennial and quasi-biennial variability in the equatorial Pacific. *Clim. Dyn*. **12**, 101-112.

Lorenz, E. M. (1956). Empirical orthogonal functions and statistical weather prediction. Technical report, Statiatical Forecast Project Report 1, Dept. of. Meteor., MIT. 49 pp.

Noguer, M. (1994). Using statistical techniques to deduce local climate distributions. An application for model validation. *Meteorol. Appl.*, **1**, 227-287.

Parker, D. E., P. D. Jones, C. K. Folland and A. Bevan (1994). Interdecadal changes of surface temperature since the late nineteenth century. *J. Geophys. Res.,* **99**, 14373–14399.

Pedlosky, J. (1987). *Goephysical Fluids Dynamics*. Springer Verlag. 710 pp.

Rogers, J. C. and H. van Loon (1979). The seesaw in winter terperatures between Greenland and Northern Europe. Part II: Some atmospheric and oceanic effects in middle and high latitudes. *Mon. Wea. Rev.*, **107**, 509-519.

Slonosky, V. C. (1999). Surface circulation variability over Europe, 1822–1995. PhD Thesis. School of Environmental Sciences, University of East Anglia, Norwich UK.

Slonosky, V. C, P. D. Jones, T. D. Davies (2001). Atmospheric circulation variability and surface temperature in Europe from the 18th century to 1995. *Int. J. Climatol.*

Tinsley, B. A. (1988). The solar cycle and the QBO influences on the latitudes of storm tracks in the North Atlantic. *Geophys. Res. Lett.* **15**, 409-412.

Valero F, Luna M Y, Martin M L (1997) An overview of a heavy rain event in southeastern Iberia: the role of large-scale meteorological conditions. Ann. Geophysicae 15: 494-502.

Van Loon, H. and J. C. Rogers (1978). The see-saw in winter temperatures between Greenland and northern Europe. Part I: General description. *Mon. Wea. Rev.*, **106**, 296-310.

Wilks, D. S. (1995). *Statistical methods in the atmospheric sciences: an introduction*. International Geophysics Series, vol 59. Academic Press. New York. 464 pp.

Yasunari T. and Seki Y. (1992). Role of the Asian Monsoon on the interannual variability of the global climate system. *J. Meteor. Soc. Japan*, **70**,177-189.

Zeng, N. and D. Neelin (2000). The role of vegetation-climate interaction and interannual variability in shaping the African Savanna. *J. Climate*, **13**, 2665-2669.